TDDFT: From optical excitations to real-time dynamics

E.K.U. Gross
Fritz Haber Center for Molecular Dynamics

האוניברסיטה העברית בירושלים
THE HEBREW UNIVERSITY OF JERUSALEM

What do we want to describe?

System in laser field:
Generic situation

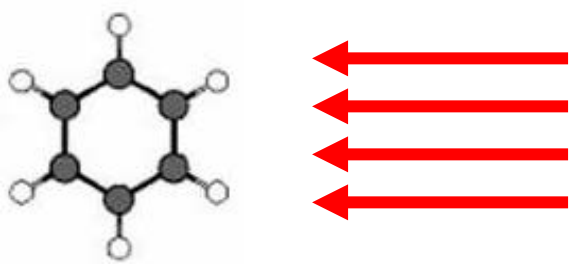

$$\hat{H}(t) = \hat{T}_e + \hat{W}_{ee} + \hat{W}_{nn} + \sum_{j,\alpha} - \frac{Z_\alpha e^2}{|r_j - R_\alpha|} + \vec{r}_j \cdot \vec{E}(t) \cdot \sin \omega t$$

What do we want to describe?

System in laser field:
Generic situation

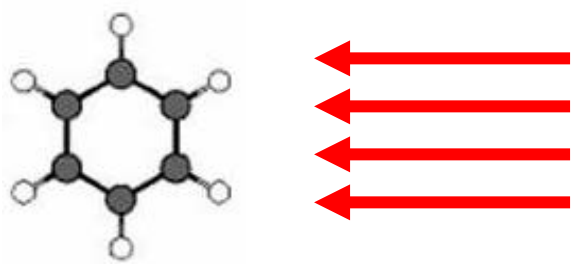

$$\hat{H}(t) = \hat{T}_e + \hat{W}_{ee} + \hat{W}_{nn} + \sum_{j,\alpha} - \frac{Z_\alpha e^2}{|r_j - R_\alpha|} + \vec{r}_j \cdot \vec{E}(t) \cdot \sin \omega t$$

Electronic transport: Generic situation

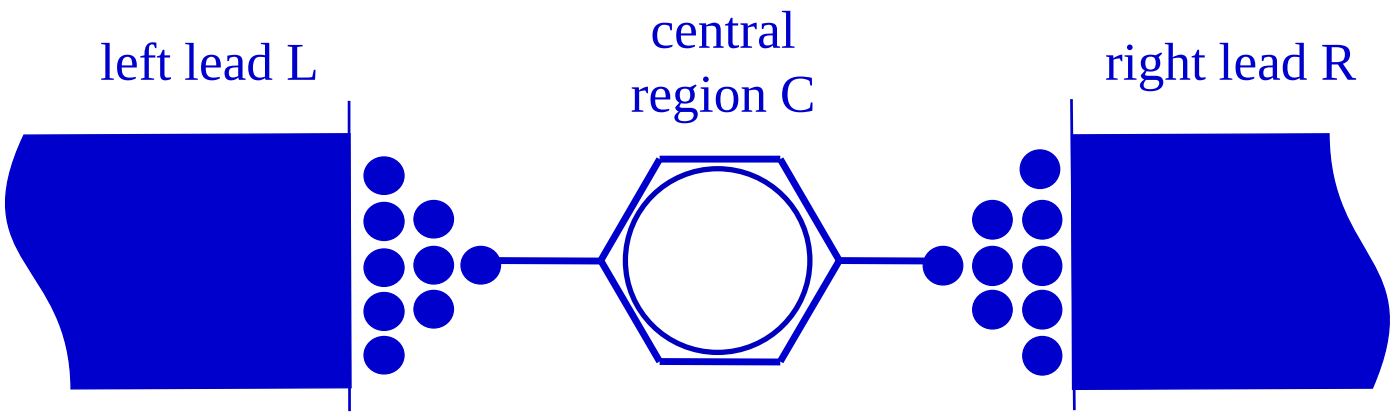

Bias between L and R is turned on: U(t) ⟶ V

$$\hat{H}(t) = \hat{T}_e + \hat{W}_{ee} + \sum_{j,\alpha} - \frac{Z_\alpha e^2}{|r_j - R_\alpha|} + \vec{r}_j \cdot \vec{E}(t) \cdot \sin \omega t$$

$$\hat{H}(t) = \hat{T}_e + \hat{W}_{ee} + \sum_{j,\alpha} - \frac{Z_\alpha e^2}{|r_j - R_\alpha|} + \vec{r}_j \cdot \vec{E}(t) \cdot \sin \omega t$$

Three important approximations lead to this Hamiltonian:

- **Nuclei treated as clamped or moving on classical trajectories R(t)**
- **Electron-photon interaction treated as classical field**
- **Non-relativistic limit**

$$\hat{H}(t) = \hat{T}_e + \hat{W}_{ee} + \sum_{j,\alpha} - \frac{Z_\alpha e^2}{|r_j - R_\alpha|} + \vec{r}_j \cdot \vec{E}(t) \cdot \sin \omega t$$

Three important approximations lead to this Hamiltonian:

- **Nuclei treated as clamped or moving on classical trajectories R(t)**
- **Electron-photon interaction treated as classical field**
- **Non-relativistic limit**

Strong laser ($v_{laser}(t) \geq v_{en}$) :

Non-perturbative solution of full TDSE required

Weak laser ($v_{laser}(t) << v_{en}$) :

Calculate 1. Linear density response $\rho_1(\vec{r}\, t)$

2. Dynamical polarizability $\alpha(\omega) = -\frac{e}{E}\int z\, \rho_1(\vec{r}, \omega) d^3r$

3. Photo-absorption cross section $\sigma(\omega) = -\frac{4\pi\omega}{c} \mathrm{Im}\, \alpha$

Photo-absorption in weak lasers

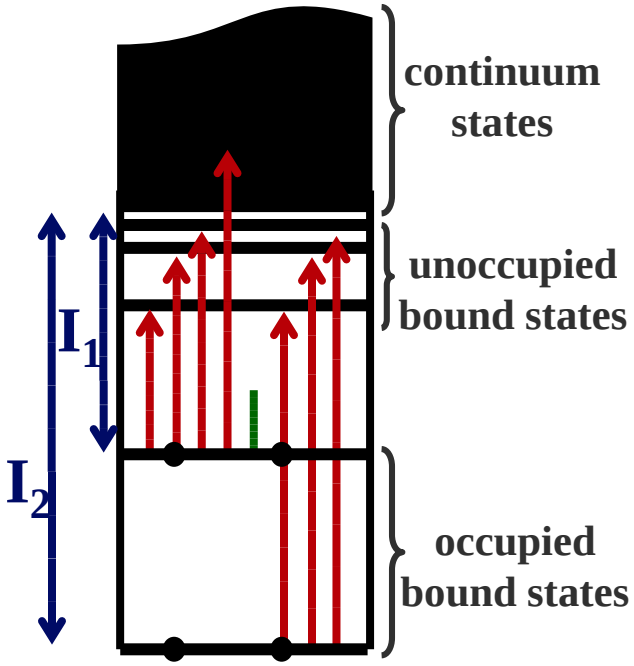

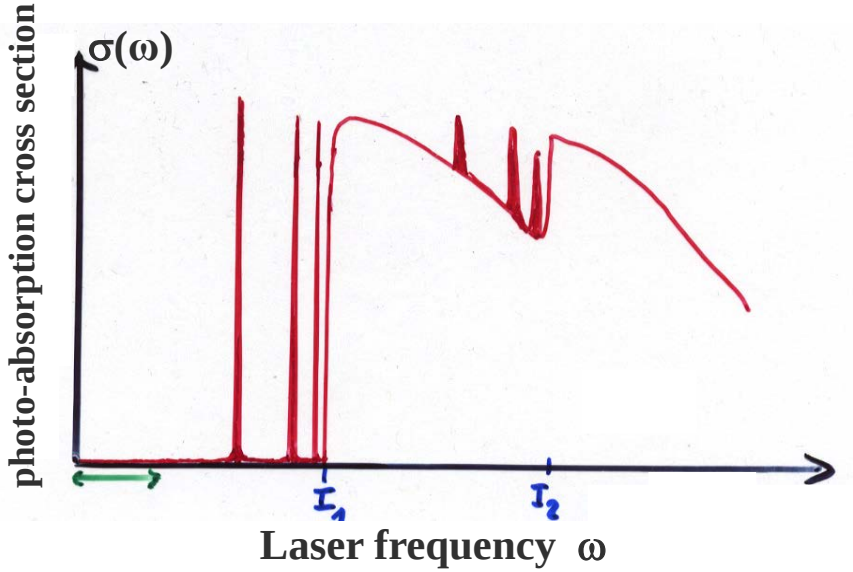

OUTLINE

- **Basic theorems of TDDFT**

- **TDDFT in the linear response regime:**
  -- Photo-absorption (optical and UV regime)

- **Real-time dynamics far from equilibrium**
  -- Laser-driven spin dynamics
  -- Transport through molecular junctions

Basic theorems of TDDFT

(E. Runge, E.K.U.G., PRL 52, 997 (1984))

1-1 correspondence (TD analogue of Hohenberg-Kohn theorem):

$$v(rt) \xleftrightarrow{1\text{-}1} \rho(rt)$$

The time-dependent density determines uniquely the time-dependent external potential and hence all physical observables for fixed initial state.

TDKS theorem:

The time-dependent density of the interacting system of interest can be calculated as density

$$\rho(rt) = \sum_{j=1}^{N} \left|\varphi_j(rt)\right|^2$$

of an auxiliary non-interacting (KS) system

$$i\hbar \frac{\partial}{\partial t}\varphi_j(rt) = \left(-\frac{\hbar^2\nabla^2}{2m} + v_S[\rho](rt)\right)\varphi_j(rt)$$

with the local potential

$$v_S\left[\rho(r't')\right](rt) = v_{ext}(rt) + \int d^3r' \frac{\rho(r't)}{|r-r'|} + v_{xc}\left[\rho(r't')\right](rt)$$

Basic theorems of TDDFT

(E. Runge, E.K.U.G., PRL 52, 997 (1984))

1-1 correspondence (TD analogue of Hohenberg-Kohn theorem):

$$v(rt) \xleftrightarrow{1\text{-}1} \rho(rt)$$

The time-dependent density determines uniquely the time-dependent external potential and hence all physical observables for fixed initial state.

TDKS theorem:

The time-dependent density of the interacting system of interest can be calculated as density

$$\rho(rt) = \sum_{j=1}^{N} \left|\varphi_j(rt)\right|^2$$

of an auxiliary non-interacting (KS) system

$$i\hbar \frac{\partial}{\partial t}\varphi_j(rt) = \left(-\frac{\hbar^2\nabla^2}{2m} + v_S[\rho](rt)\right)\varphi_j(rt)$$

with the local potential

$$v_S\left[\rho(r't')\right](rt) = v_{ext}(rt) + \int d^3r' \frac{\rho(r't)}{|r-r'|} + v_{xc}\left[\rho(r't')\right](rt)$$

Proof of the 1-1 correspondence between $v(\vec{r}\,t)$ and $\rho(\vec{r}\,t)$

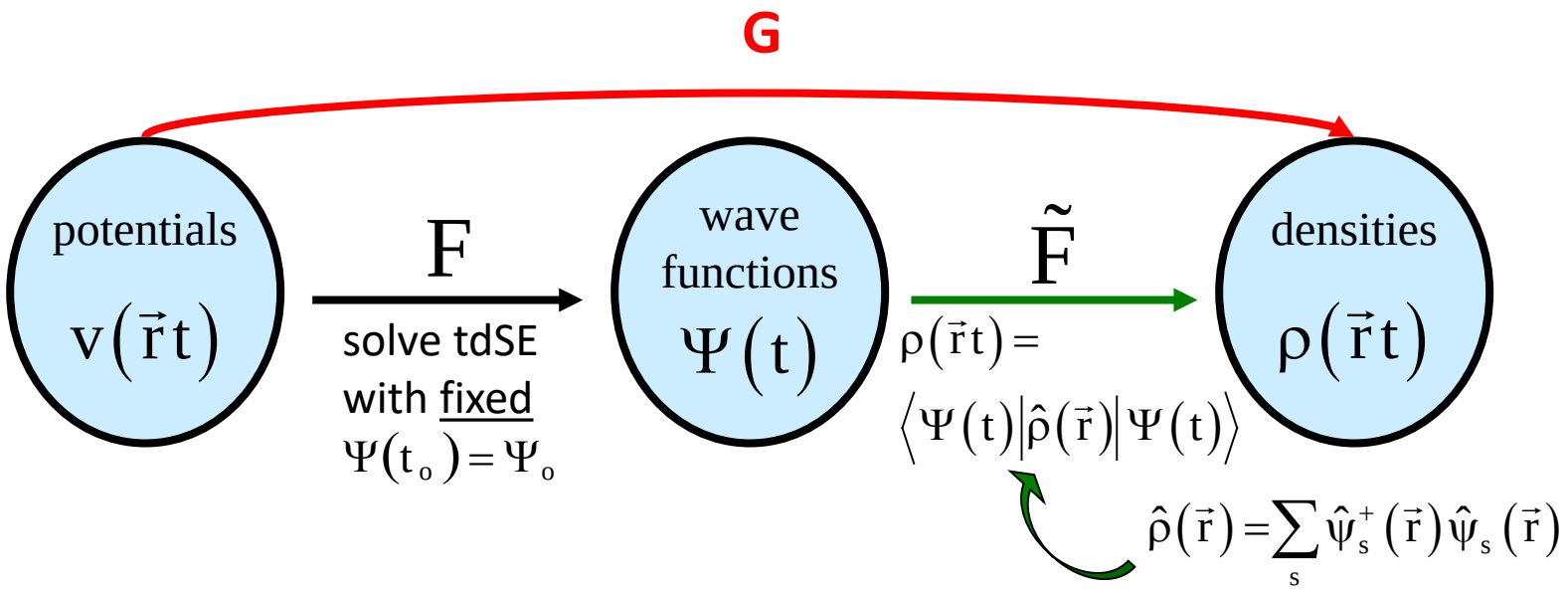

to be shown that

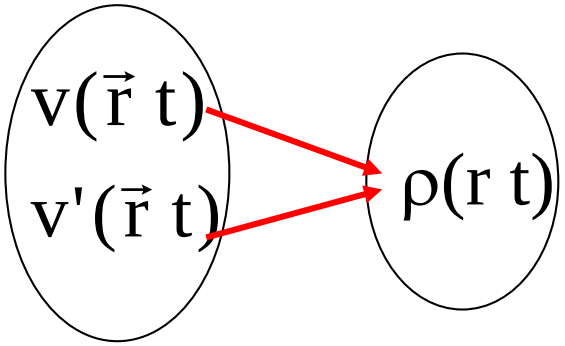

is impossible

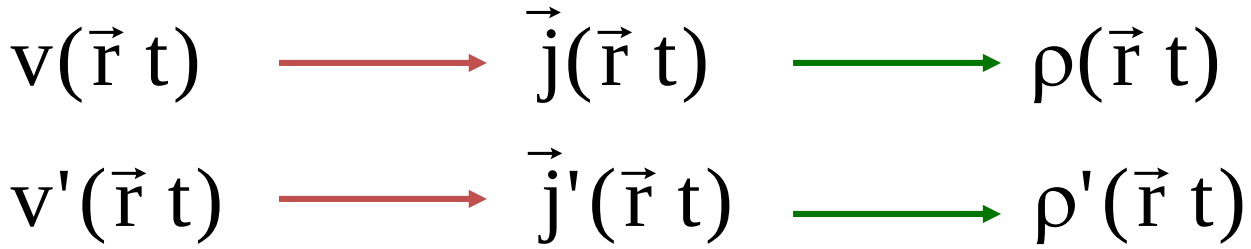
v(r t)
j(r t)
ρ(r t)
v'(r t)
j'(r t)
ρ'(r t)

$$v(\vec{r}\,t) \longrightarrow \vec{j}(\vec{r}\,t) \longrightarrow \rho(\vec{r}\,t)$$

$$v'(\vec{r}\,t) \longrightarrow \vec{j}'(\vec{r}\,t) \longrightarrow \rho'(\vec{r}\,t)$$

use

$$i\frac{\partial \vec{j}(\vec{r},t)}{\partial t} = \left\langle \Psi(t) \left| \left[\hat{j}(\vec{r}) \, , \, \hat{H}(t) \right] \right| \Psi(t) \right\rangle$$

equation of motion for $\vec{j}$

and

$$\frac{\partial \rho(\vec{r},t)}{\partial t} = - \operatorname{div} j(\vec{r},t)$$

continuity equation

to show that ρ and ρ' will become different from each other infinitesimally later than t_0

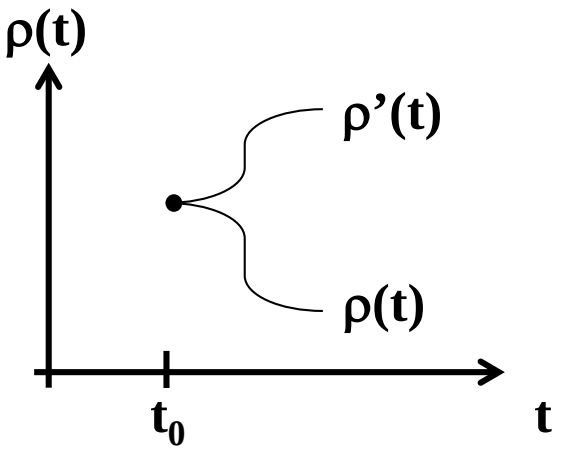

Simplest possible approximation for $v_{xc}[\rho](\vec{r}t)$

Adiabatic Local Density Approximation (ALDA)

$$v_{xc}^{ALDA}(\vec{r}\,t) := v_{xc,stat}^{hom}(n)\Big|_{n=\rho(\vec{r}\,t)}$$

$v_{xc,stat}^{hom}$ **= xc potential of static homogeneous e-gas**

Simplest possible approximation for $v_{xc}[\rho](\vec{r}t)$

Adiabatic Local Density Approximation (ALDA)

$$v_{xc}^{ALDA}(\vec{r}\,t) := v_{xc,stat}^{hom}(n)\Big|_{n=\rho(\vec{r}\,t)}$$

$v_{xc,stat}^{hom}$ **= xc potential of static homogeneous e-gas**

Any approximate ground-state-DFT xc functional can be used to generate an adiabatic approximation for TDDFT

$$v_{xc}^{adiab}(\vec{r}\,t) := v_{xc,GS}^{approx}[n]\Big|_{n=\rho(\vec{r}\,t)}$$

LINEAR RESPONSE THEORY

$t = t_0$: Interacting system in ground state of potential $v_0(r)$ with density $\rho_0(r)$

$t > t_0$: Switch on perturbation $v_1(r\,t)$ (with $v_1(r\,t_0)=0$).

Density: $\rho(r\,t) = \rho_0(r) + \delta\rho(r\,t)$

Consider functional $\rho[v](r\,t)$ defined by solution of interacting TDSE

Functional Taylor expansion of $\rho[v]$ around v_o:

$$\rho[v](r\,t) = \rho[v_0 + v_1\,](r\,t)$$

$$= \rho[v_0\,](r\,t) \longrightarrow \rho_o(r)$$

$$+ \int \left.\frac{\delta\rho[v](r\,t)}{\delta v(r'\,t')}\right|_{v_0} v_1(r'\,t')\,d^3r'\,dt' \longrightarrow \rho_1(r\,t)$$

$$+ \frac{1}{2}\int\int \left.\frac{\delta^2\rho[v](r\,t)}{\delta v(r'\,t')\delta v(r''\,t'')}\right|_{v_0} v_1(r',t')v_1(r'',t'')\,d^3r'\,d^3r''\,dt'\,dt'' \longrightarrow \rho_2(r\,t)$$

$$\vdots$$

$\rho_1(r,t)$ = linear density response of interacting system

$$\chi(r\,t, r'\,t') := \left.\frac{\delta\rho[v](r\,t)}{\delta v(r'\,t')}\right|_{v_0}$$ = density-density response function of interacting system

Lehmann representation of the full response function

$$\chi(r, r'; \omega) = \lim_{\eta\to 0^+} \sum_m \left(\frac{\langle 0|\hat\rho(r)|m\rangle\langle m|\hat\rho(r')|0\rangle}{\omega - (E_m - E_0) + i\eta} - \frac{\langle 0|\hat\rho(r')|m\rangle\langle m|\hat\rho(r)|0\rangle}{\omega + (E_m - E_0) + i\eta} \right)$$

with the exact many-body eigenfunctions and energies of the initial unperturbed interacting system Hamiltnian $H(t_0)|m\rangle = E_m|m\rangle$

$\Rightarrow$ The exact linear density response

$$\rho_1(\omega) = \chi(\omega)\, v_1$$

has poles at the exact excitation energies $\Omega = E_m - E_0$

Analogous functional $\rho_s[v_s](r\,t)$ for <u>non</u>-interacting system

$$\rho_S[v_S](r\,t) = \rho_S[v_{S,0} + v_{S,1}](r\,t) = \rho_S[v_{S,0}](r\,t) + \int \left.\frac{\delta\rho_S[v_S](r\,t)}{\delta v_S(r'\,t')}\right|_{v_{S,0}} v_{S,1}(r'\,t')\, d^3r'\,dt' + \cdots$$

$$\chi_S(r\,t, r'\,t') := \left.\frac{\delta\rho_S[v_S](r\,t)}{\delta v_S(r'\,t')}\right|_{v_{S,0}} \quad = \quad \textbf{density-density response function of } \underline{\textbf{non}}\textbf{-interacting system}$$

χ_S (r,r',ω) has also poles as function of ω, but at the non-interacting single-particle (KS) excitation energies.

GOAL: **Find a way to calculate $\rho_1(r\,t)$ without explicitly evaluating $\chi(r\,t,r't')$ of the interacting system**

starting point: **Definition of xc potential**

$$v_{xc}[\rho](r\,t) := v_S[\rho](r\,t) - v_{ext}[\rho](r\,t) - v_H[\rho](r\,t)$$

v_{xc} is well-defined through the non-interacting and the interacting 1-1 mapping.

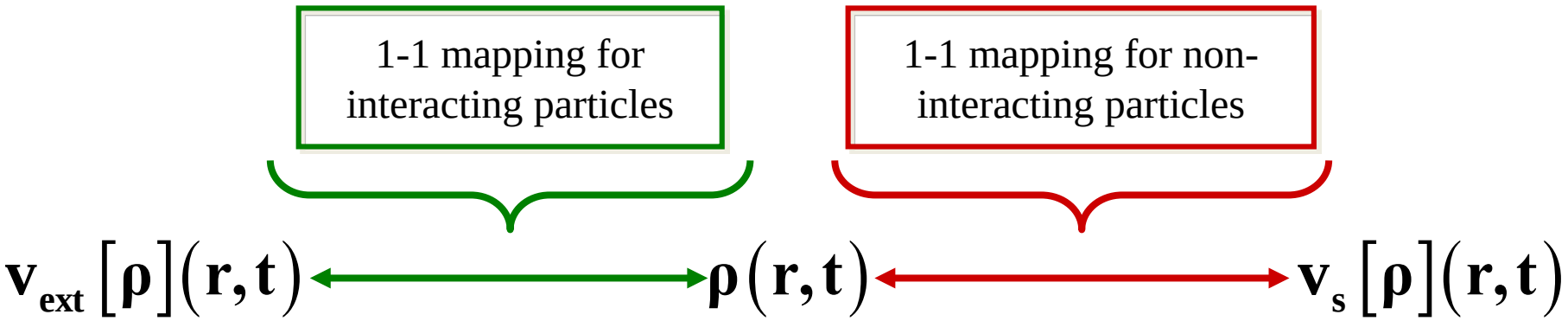

$$\left.\frac{\delta v_{xc}[\rho](r\,t)}{\delta\rho(r'\,t')}\right|_{\rho_0} = \left.\frac{\delta v_{S}[\rho](r\,t)}{\delta\rho(r'\,t')}\right|_{\rho_0} - \left.\frac{\delta v_{ext}[\rho](r\,t)}{\delta\rho(r'\,t')}\right|_{\rho_0} - \frac{\delta(t-t')}{|r-r'|}$$

$$\left.\frac{\delta v_{xc}[\rho](r\,t)}{\delta\rho(r'\,t')}\right|_{\rho_0} = \left.\frac{\delta v_S[\rho](r\,t)}{\delta\rho(r'\,t')}\right|_{\rho_0} - \left.\frac{\delta v_{ext}[\rho](r\,t)}{\delta\rho(r'\,t')}\right|_{\rho_0} - \frac{\delta(t-t')}{|r-r'|}$$

$$\uparrow \qquad\qquad \uparrow \qquad\qquad \uparrow \qquad\qquad \uparrow$$

$$f_{xc}(r\,t, r'\,t') \qquad \chi_S^{-1}(r\,t, r'\,t') \qquad \chi^{-1}(r\,t, r'\,t') \qquad W_C(r\,t, r'\,t')$$

$$\left.\frac{\delta v_{xc}[\rho](r\,t)}{\delta\rho(r'\,t')}\right|_{\rho_0} = \left.\frac{\delta v_S[\rho](r\,t)}{\delta\rho(r'\,t')}\right|_{\rho_0} - \left.\frac{\delta v_{ext}[\rho](r\,t)}{\delta\rho(r'\,t')}\right|_{\rho_0} - \frac{\delta(t-t')}{|r-r'|}$$

$$\uparrow \qquad\qquad \uparrow \qquad\qquad \uparrow \qquad\qquad \uparrow$$

$$f_{xc}(r\,t,r'\,t') \qquad \chi_S^{-1}(r\,t,r'\,t') \qquad \chi^{-1}(r\,t,r'\,t') \qquad W_C(r\,t,r'\,t')$$

$$f_{xc} + W_C = \chi_S^{-1} - \chi^{-1}$$

$$\left.\frac{\delta v_{xc}[\rho](r\,t)}{\delta\rho(r'\,t')}\right|_{\rho_0} = \left.\frac{\delta v_S[\rho](r\,t)}{\delta\rho(r'\,t')}\right|_{\rho_0} - \left.\frac{\delta v_{ext}[\rho](r\,t)}{\delta\rho(r'\,t')}\right|_{\rho_0} - \frac{\delta(t-t')}{|r-r'|}$$

$$\uparrow \qquad\qquad \uparrow \qquad\qquad \uparrow \qquad\qquad \uparrow$$

$$f_{xc}(r\,t, r'\,t') \qquad \chi_S^{-1}(r\,t, r'\,t') \qquad \chi^{-1}(r\,t, r'\,t') \qquad W_C(r\,t, r'\,t')$$

$$\chi_S \bullet \left| f_{xc} + W_C = \chi_S^{-1} - \chi^{-1} \right| \bullet \chi$$

$$\left.\frac{\delta v_{xc}[\rho](r\,t)}{\delta\rho(r'\,t')}\right|_{\rho_0} = \left.\frac{\delta v_S[\rho](r\,t)}{\delta\rho(r'\,t')}\right|_{\rho_0} - \left.\frac{\delta v_{ext}[\rho](r\,t)}{\delta\rho(r'\,t')}\right|_{\rho_0} - \frac{\delta(t-t')}{|r-r'|}$$

$$\uparrow \qquad\qquad \uparrow \qquad\qquad \uparrow \qquad\qquad \uparrow$$

$$f_{xc}(r\,t, r'\,t') \qquad \chi_S^{-1}(r\,t, r'\,t') \qquad \chi^{-1}(r\,t, r'\,t') \qquad W_C(r\,t, r'\,t')$$

$$\chi_S \bullet \left| f_{xc} + W_C = \chi_S^{-1} - \chi^{-1} \right| \bullet \chi$$

$$\chi_S (f_{xc} + W_C)\chi = \chi - \chi_S$$

$$\chi = \chi_S + \chi_S \left(W_{ee} + f_{xc} \right) \chi$$

Act with this operator equation on arbitrary $v_1(r\,t)$ and use $\chi\, v_1 = \rho_1$:

$$\rho_1(r\,t) = \int d^3r'dt' \chi_S(r\,t, r't') \left[v_1(r\,t) + \int d^3r''dt'' \left\{ W_{ee}(r't', r''t'') + f_{xc}(r't', r''t'') \right\} \rho_1(r''t'') \right]$$

- Exact integral equation for $\rho_1(r\,t)$, to be solved iteratively
- Need approximation for $f_{xc}(r't', r''t'') = \left. \frac{\delta v_{xc}[\rho](r't')}{\delta \rho(r''t'')} \right|_{\rho_0}$
  (either for f_{xc} directly or for v_{xc})

Total photoabsorption cross section of the Xe atom versus photon energy in the vicinity of the 4d threshold.

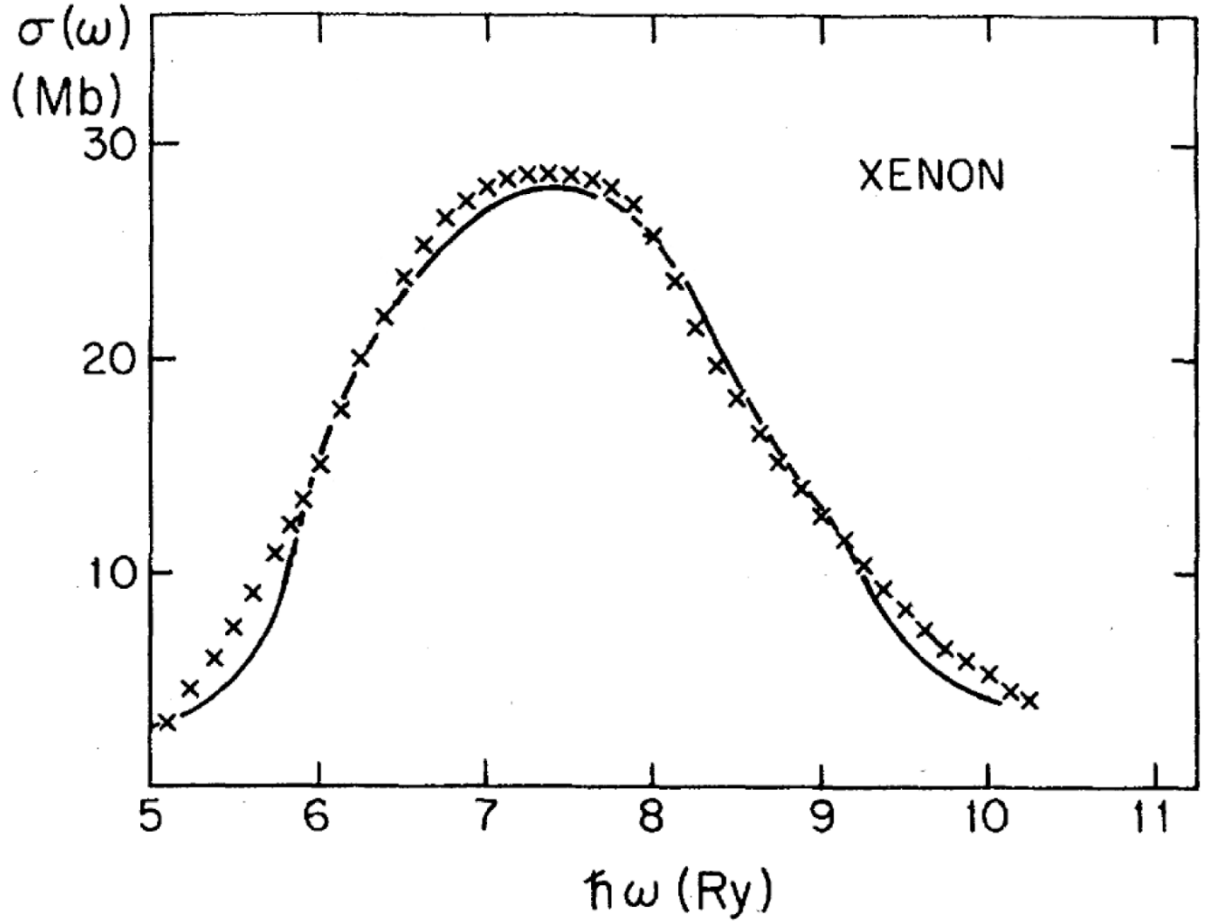

Solid line: self-consistent time-dependent KS calculation [A. Zangwill and P. Soven, Phys. Rev. A 21, 1561 (1980)]; crosses: experimental data [R. Haensel, G. Keitel, P. Schreiber, and C. Kunz, Phys. Rev. 188, 1375 (1969)].

Photo-absorption in weak lasers

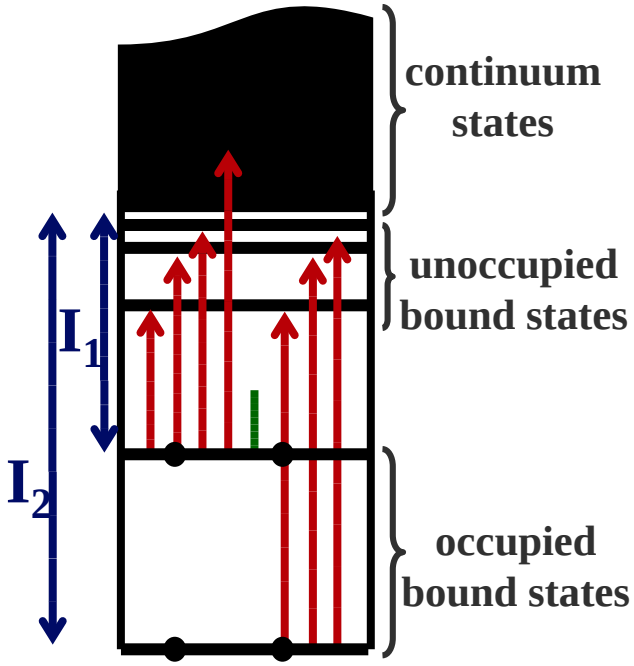

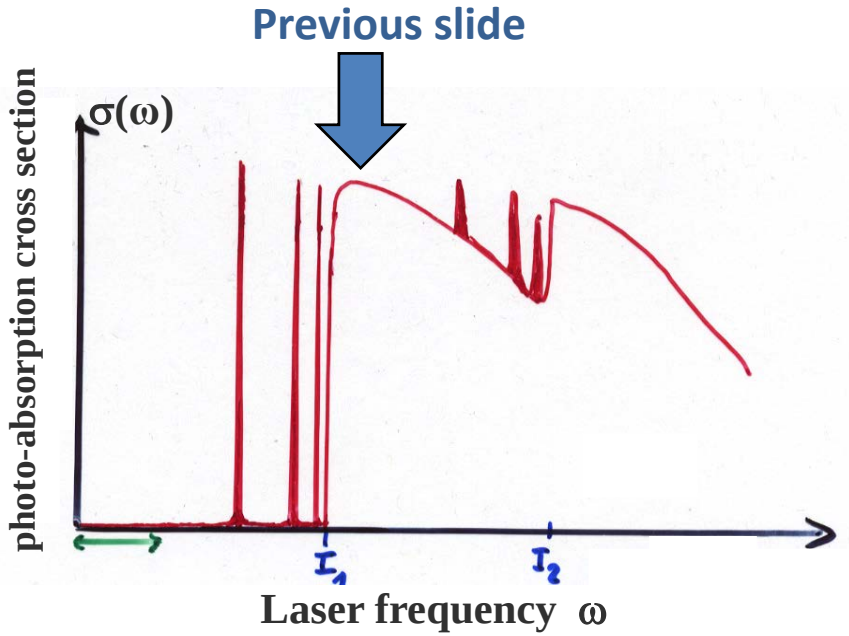

Photo-absorption in weak lasers

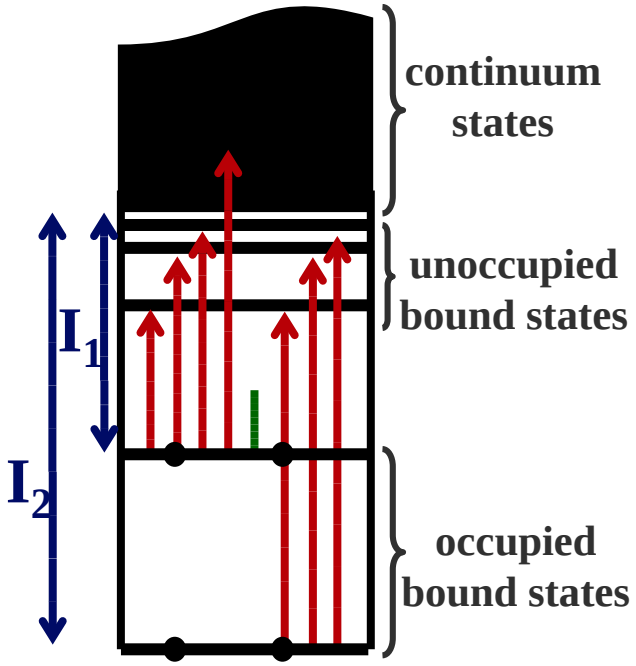

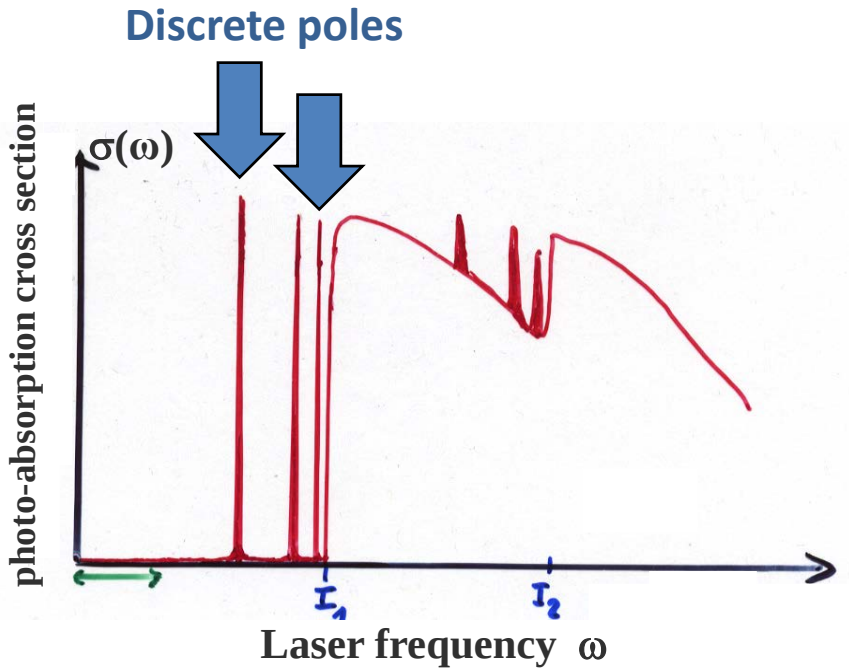

Looking at those frequencies, Ω, for which $\rho_1(\omega)$ has poles, leads to a (non-linear) eigenvalue equation

M. Petersilka, U. J. Gossmann, E.K.U.G., PRL 76, 1212 (1996)
T. Grabo, M. Petersilka, EKUG, J. Mol. Struc. (Theochem) 501, 353 (2000)
M.E. Casida, Recent Advances in Density Functional Methods I, 155 (1996)

$$\sum_{q'}\left(A_{qq'}(\Omega)+\omega_q\delta_{qq'}\right)\beta_{q'}=\Omega\beta_q$$

where

$$A_{qq'}=\alpha_{q'}\int d^3r\int d^3r'\,\Phi_q(r)\left(\frac{1}{|r-r'|}+f_{xc}(r,r',\Omega)\right)\Phi_{q'}(r')$$

$q=(j,a)$ double index $\qquad \alpha_q=f_a-f_j$

$\Phi_q(r)=\varphi_a^*(r)\varphi_j(r) \qquad \omega_q=\varepsilon_a-\varepsilon_j$

Atom	Experimental Excitation Energies $^1S \rightarrow {}^1P$ (in Ry)	KS energy differences $\Delta\epsilon_{KS}$ (Ry)	TDDFT
Be	0.388	0.259	0.391
Mg	0.319	0.234	0.327
Ca	0.216	0.157	0.234
Zn	0.426	0.315	0.423
Sr	0.198	0.141	0.210
Cd	0.398	0.269	0.391

from: M. Petersilka, U. J. Gossmann, E.K.U.G., PRL 76, 1212 (1996)

Excitation energies of CO molecule [mH]

State	$\Omega_{\text{expt KS}}$	KS-transition	$\Delta\epsilon_{KS}$	TDDFT
$A\ ^1\Pi$	312.7	$5\sigma \rightarrow 2\pi$	252.3	310.2
$a\ ^3\Pi$	232.3			221.4
$I\ ^1\Sigma^-$	363.1	$1\pi \rightarrow 2\pi$	362.6	362.6
$e\ ^3\Sigma^-$	363.1			362.6
$a'\ ^3\Sigma^+$	312.7			314.9
$D\ ^1\Delta$	375.9			380.7
$d\ ^3\Delta$	344.0			339.6

Molecular excitation energies from time-dependent density-functional theory
T Grabo, M Petersilka, EKU Gross, J Mol Struc-Theochem 501, 353 (2000).

Failures of ALDA in the linear response regime

- **H_2 dissociation is incorrect:**

$$E\left(^1\Sigma_u^+\right) - E\left(^1\Sigma_g^+\right) \xrightarrow[R\to\infty]{} 0 \quad \textbf{(in ALDA)}$$

(see: Gritsenko, van Gisbergen, Görling, Baerends, J. Chem. Phys. 113, 8478 (2000))

- **response of long chains strongly overestimated**

(see: Champagne et al., J. Chem. Phys. 109, 10489 (1998) and 110, 11664 (1999))

- **in periodic solids,** $f_{xc}^{ALDA}(q,\omega,\rho) = c(\rho)$ **whereas,**

for insulators, $f_{xc}^{exact} \xrightarrow[q\to 0]{} 1/q^2$ **divergent.**

- **charge-transfer excitations not properly described**

(see: Dreuw et al., J. Chem. Phys. 119, 2943 (2003))

Failures of ALDA in the linear response regime

- **H_2 dissociation is incorrect:**

$$E\left(^1\Sigma_u^+\right) - E\left(^1\Sigma_g^+\right) \xrightarrow[R\to\infty]{} 0 \quad \textbf{(in ALDA)}$$

(see: Gritsenko, van Gisbergen, Görling, Baerends, J. Chem. Phys. 113, 8478 (2000))

- **response of long chains strongly overestimated**

(see: Champagne et al., J. Chem. Phys. 109, 10489 (1998) and 110, 11664 (1999))

- **in periodic solids,** $f_{xc}^{ALDA}(q,\omega,\rho) = c(\rho)$ **whereas,**

for insulators, $f_{xc}^{exact} \xrightarrow[q\to 0]{} 1/q^2$ **divergent.**

- **charge-transfer excitations not properly described**

(see: Dreuw et al., J. Chem. Phys. 119, 2943 (2003))

These difficulties have largely been solved by xc functionals more advanced than ALDA

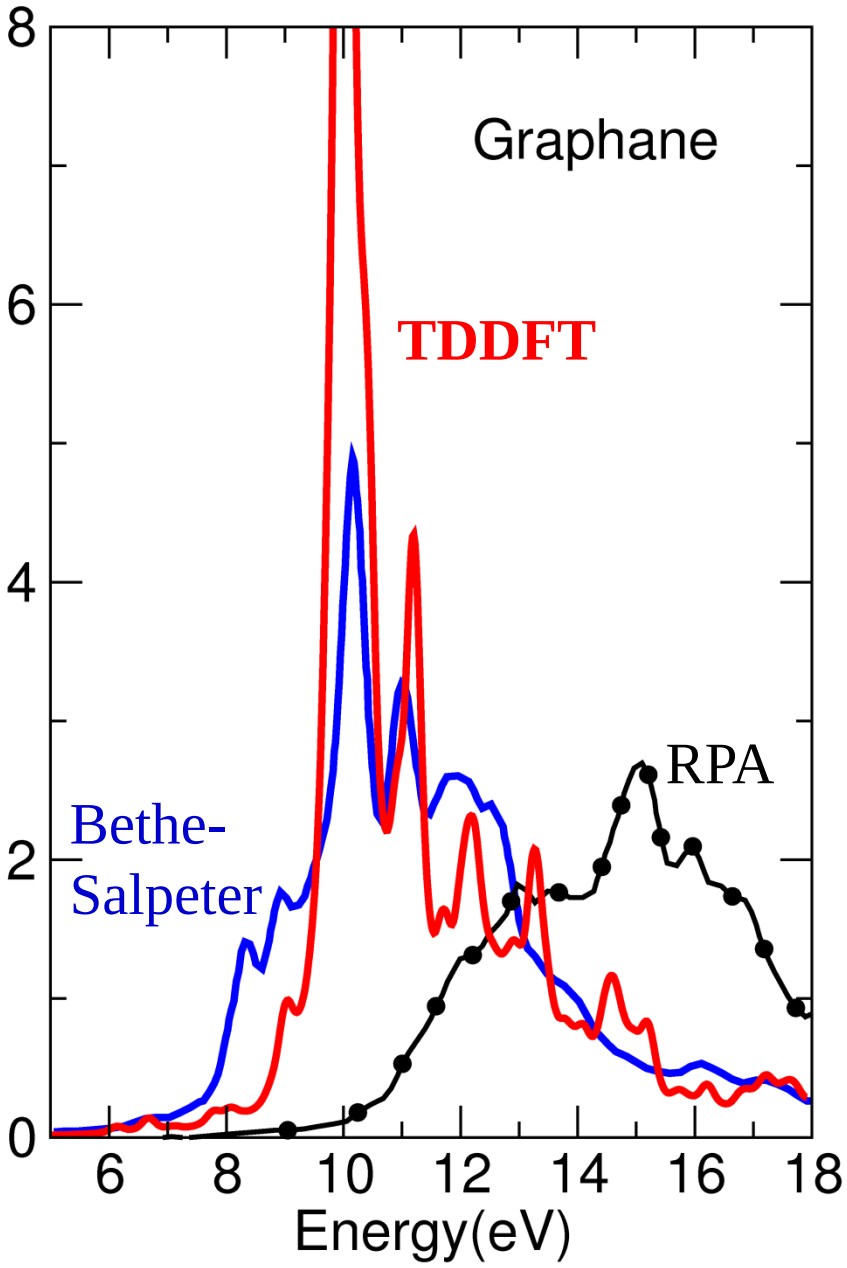

Approximate functional used for fxc:

Bootstrap kernel:

(Sharma, Dewhurst, Sanna, EKUG, PRL **107**, 186401 (2011))

PPV

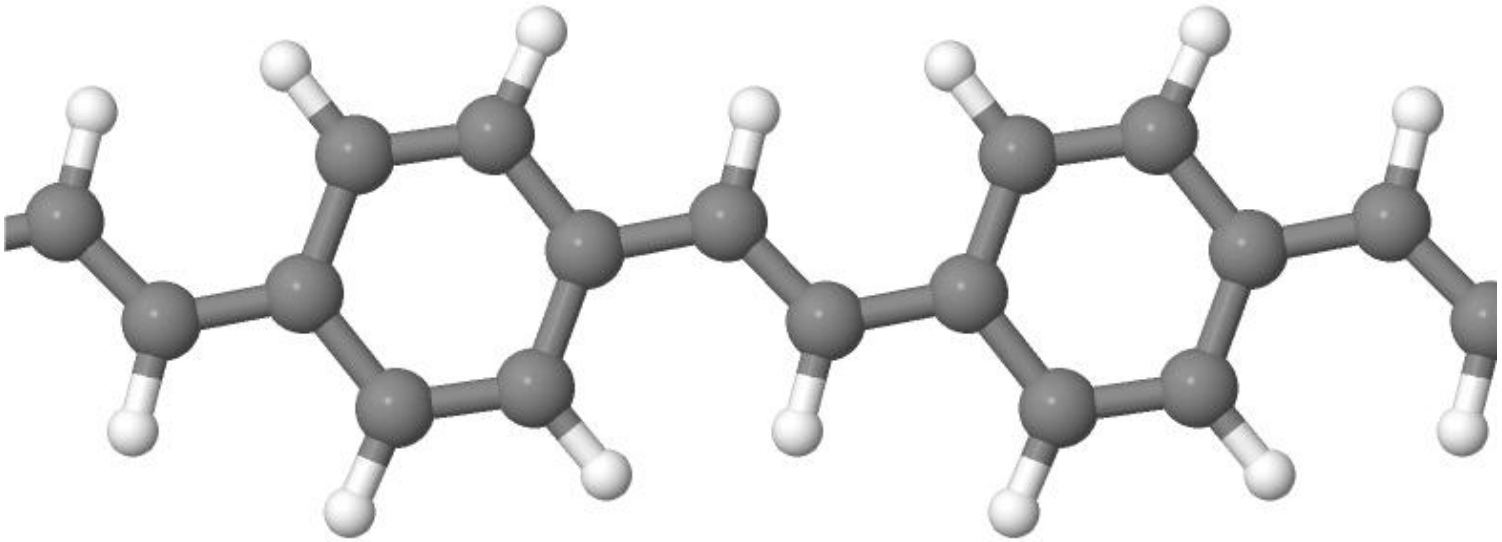

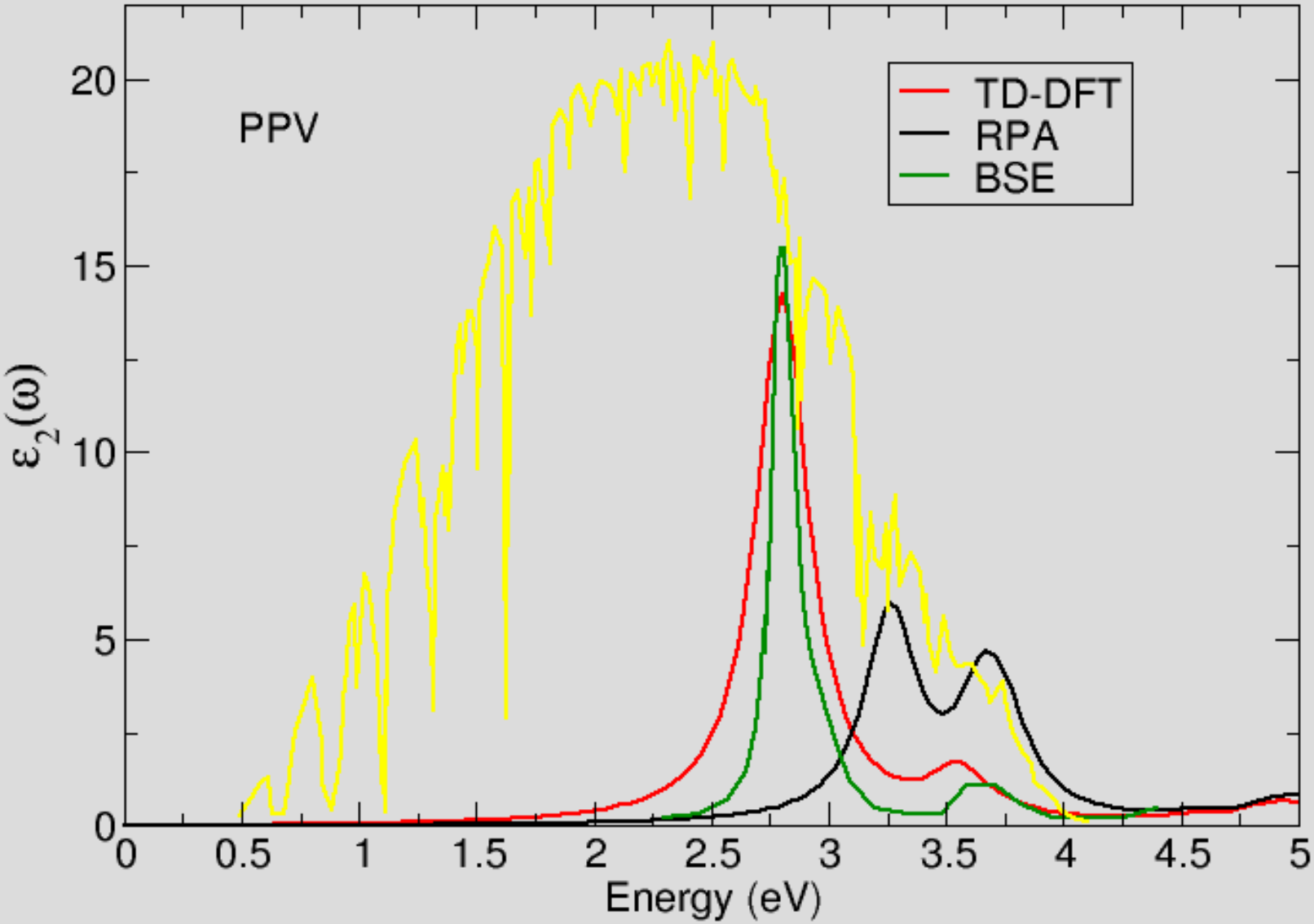
PPV
TD-DFT
RPA
BSE
$\varepsilon_2(\omega)$
Energy (eV)
0
5
10
15
20
0
0.5
1
1.5
2
2.5
3
3.5
4
4.5
5

PBTTT

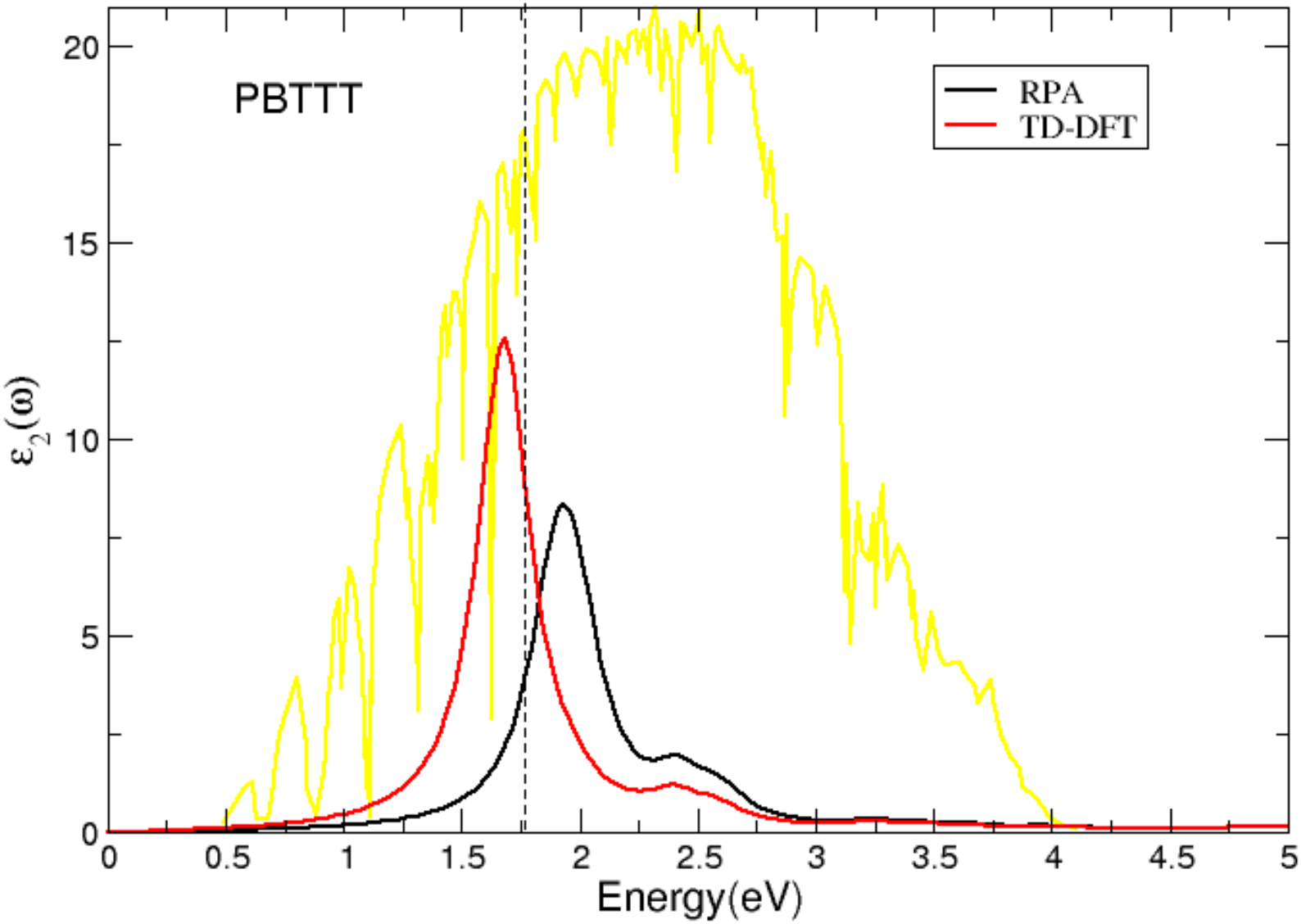
PBTTT
RPA
TD-DFT
$\varepsilon_2(\omega)$
Energy(eV)
0
5
10
15
20
0
0.5
1
1.5
2
2.5
3
3.5
4
4.5
5

Linear-response TDDFT is now being used to predict and to interpret experimental optical spectra in essentially all corners of physics and chemistry.

Some examples:

Inorganic Chemistry

Article

pubs.acs.org/IC

Luminescent Properties of Metal–Organic Framework MOF-5: Relativistic Time-Dependent Density Functional Theory Investigations

Min Ji, Xin Lan, Zhenping Han, Ce Hao,* and Jieshan Qiu

State Key Laboratory of Fine Chemicals, School of Chemical Engineering, Dalian University of Technology, Dalian 116024, Liaoning, China

ABSTRACT: The electronically excited state and luminescence property of metal–organic framework MOF-5 were investigated using relativistic density functional theory (DFT) and time-dependent DFT (TDDFT). The geometry, IR spectra, and UV–vis spectra of MOF-5 in the ground state were calculated using relativistic DFT, leading to good agreement between the experimental and theoretical results. The frontier molecular orbitals and electronic configuration indicated that the luminescence mechanism in MOF-5 follows ligand-to-ligand charge transfer (LLCT), namely, $\pi^* \rightarrow \pi$, rather than emission with the ZnO quantum dot (QD) proposed by Bordiga et al. The geometry and IR spectra of MOF-5 in the electronically excited state have been calculated using the relativistic TDDFT and compared with those for the ground state. The comparison reveals that the Zn_4O_{13} QD is rigid, whereas the ligands BDC^{2-} are nonrigid. In addition, the calculated emission band of MOF-5 is in good agreement with the experimental result and is similar to that of the ligand H_2BDC. The combined results confirmed that the luminescence mechanism for MOF-5 should be LLCT with little mixing of the ligand-to-metal charge transfer. The reason for the MOF-5 luminescence is explained by the excellent coplanarity between the six-membered ring consisting of zinc, oxygen, carbon, and the benzene ring.

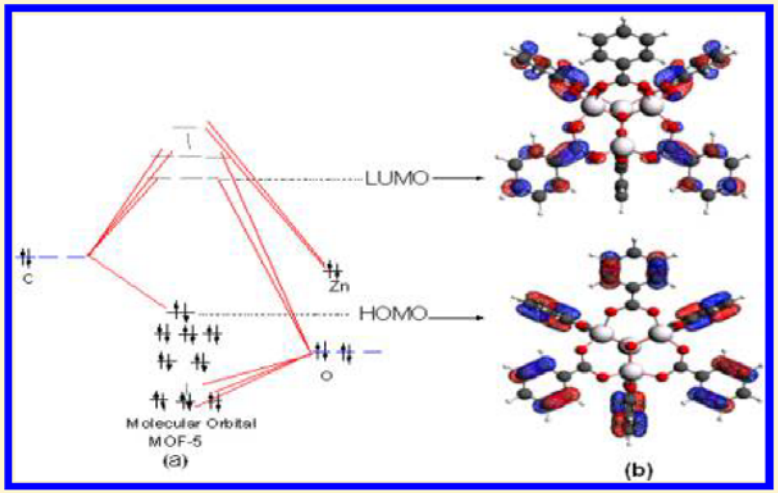

A NANOPLASMONIC SWITCH BASED ON MOLECULAR MACHINES

Yue Bing Zheng[1], *Ying-Wei Yang*[2], *Lasse Jensen*[1], *Lei Fang*[2], *Bala Krishna Juluri*[1], *Paul S. Weiss*[1], *J. Fraser Stoddart*[2], *Tony Jun Huang*[1*]

[1]The Pennsylvania State University, University Park, Pennsylvania 16802 USA

[2]Northwestern University, Evanston, Illinois 60208 USA

ABSTRACT

We aim to develop a molecular-machine-driven nanoplasmonic switch for its use in future nanophotonic integrated circuits (ICs) that have applications in optical communication, information processing, biological and chemical sensing. Experimental data show that an Au nanodisk array, coated with rotaxane molecular machines, switches its localized surface plasmon resonances (LSPR) reversibly when it is exposed to chemical oxidants and reductants. Conversely, bare Au nanodisks and disks coated with mechanically inert control compounds, do not display the same switching behavior. Along with calculations based on time-dependent density functional theory (TDDFT), these observations suggest that the nanoscale movements within surface-bound "molecular machines" can be used as the active components in plasmonic devices.

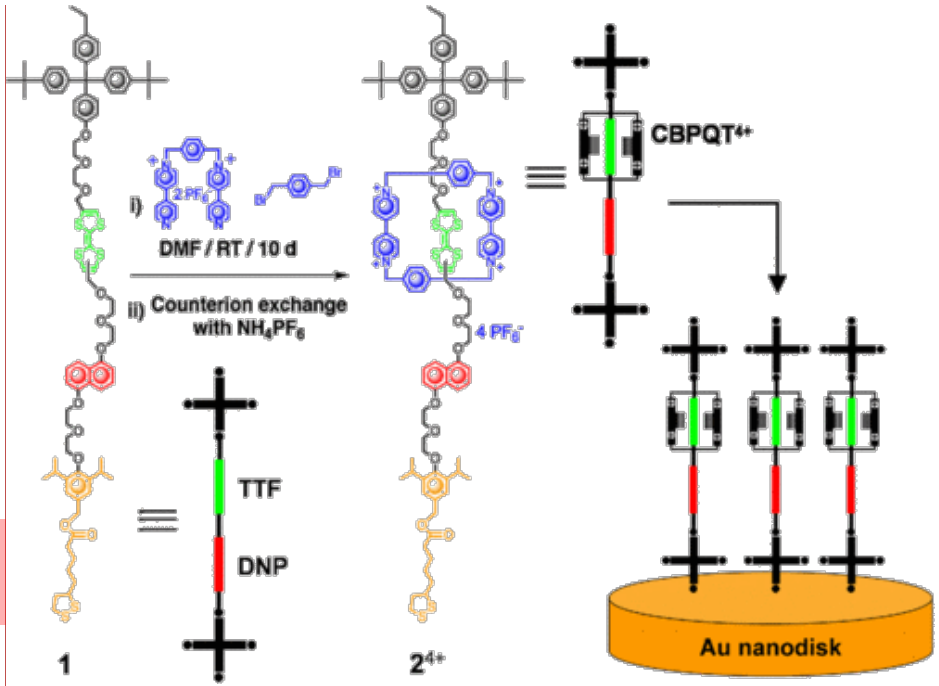

DOI: 10.1109/SENSOR.2009.5285604

Cite this: *Phys. Chem. Chem. Phys.*, 2011, **13**, 10475–10490

www.rsc.org/pccp

PAPER

First-principles calculation of electronic spectra of light-harvesting complex II†

Carolin König and Johannes Neugebauer*

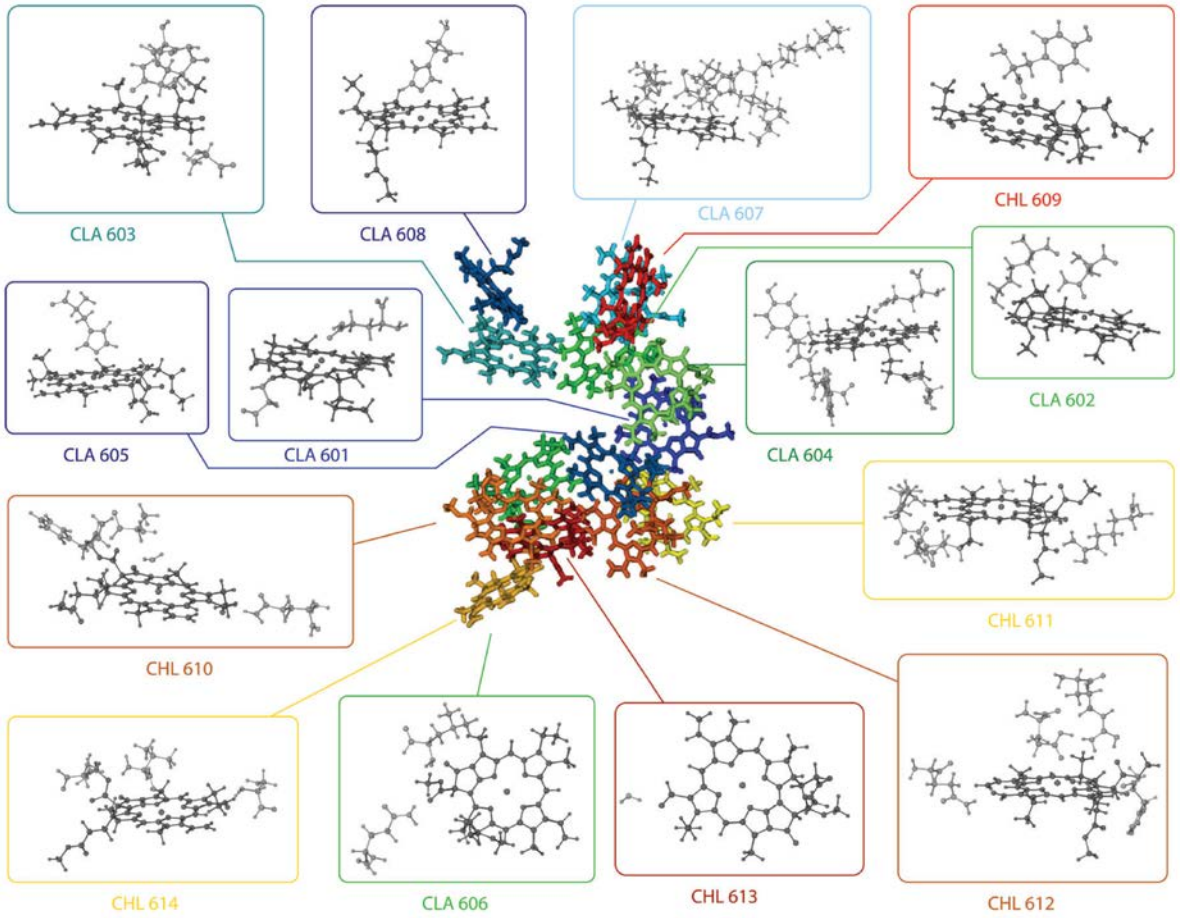

Beyond the linear regime: Real-time TDDFT prediction of electron dynamics far from equilibrium

Laser-induced spin dynamics in solids: Some predictions from real-time TDDFT

OUTLINE

- **Laser-induced demagnetisation (~ 50 fs)**
  found experimentally in 1996,
  explained by TDDFT in 2015

- **XC functionals for non-collinear magnetism**

- **Optically Induced Spin TRansfer OISTR (~ 5 fs)**
  predicted by TDDFT in 2016
  found experimentally in 2018

First experiment on ultrafast laser induced demagnetization

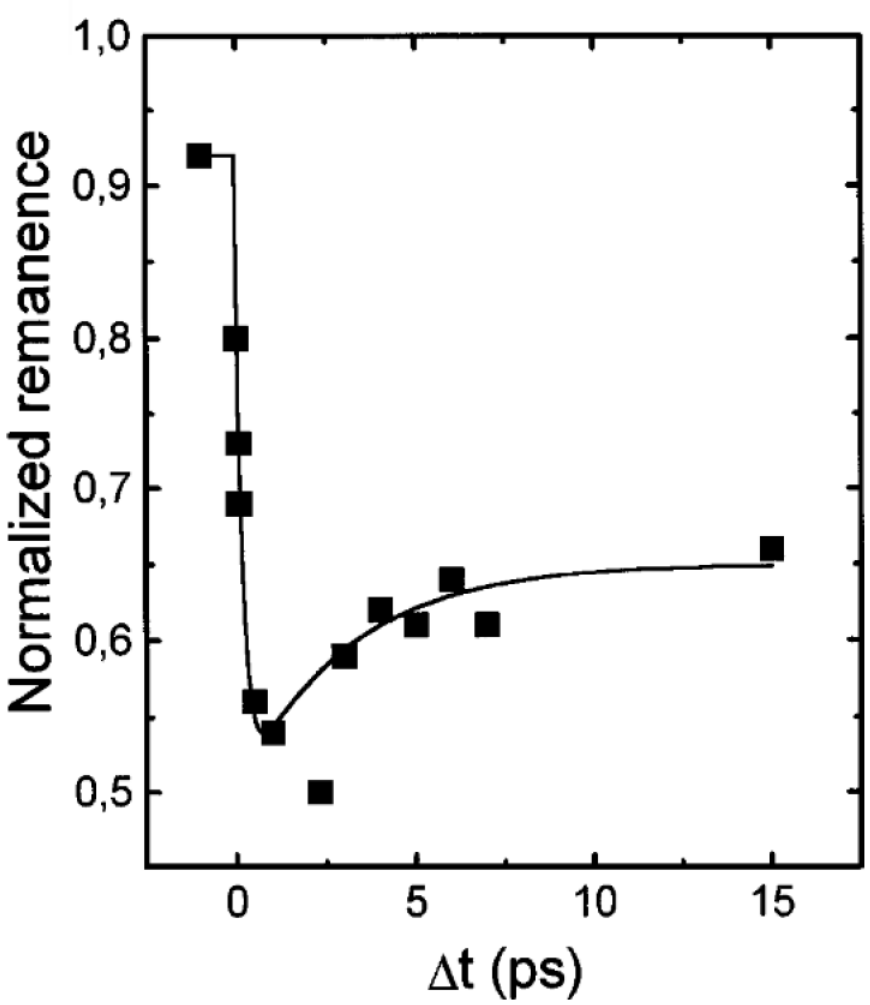

Beaurepaire et al, PRL 76, 4250 (1996)

Possible mechanisms for demagnetisation

- Direct interaction of spins with the magnetic component of the laser
  Zhang, Huebner, PRL **85**, 3025 (2000)

Possible mechanisms for demagnetisation

- Direct interaction of spins with the magnetic component of the laser
  Zhang, Huebner, PRL **85**, 3025 (2000)

- Spin-flip electron-phonon scattering
  (ultimately leading to transfer of spin angular momentum to the lattice)
  Koopmans et al, PRL **95**, 267207 (2005)

Possible mechanisms for demagnetisation

- Direct interaction of spins with the magnetic component of the laser
  Zhang, Huebner, PRL **85**, 3025 (2000)

- Spin-flip electron-phonon scattering
  (ultimately leading to transfer of spin angular momentum to the lattice)
  Koopmans et al, PRL **95**, 267207 (2005)

- Super-diffusive spin transport
  Battiato, Carva, Oppeneer, PRL **105**, 027203 (2010)

Possible mechanisms for demagnetisation

- Direct interaction of spins with the magnetic component of the laser
  Zhang, Huebner, PRL **85**, 3025 (2000)

- Spin-flip electron-phonon scattering
  (ultimately leading to transfer of spin angular momentum to the lattice)
  Koopmans et al, PRL **95**, 267207 (2005)

- Super-diffusive spin transport
  Battiato, Carva, Oppeneer, PRL **105**, 027203 (2010)

- **Our proposal for the first 50 fs:**
  Laser-induced charge excitation followed by spin-orbit-driven demagnetization of the initially not excited electrons

Quantity of prime interest:

vector field of spin magnetization

$\vec{m}(\vec{r}, t)$

Quantity of prime interest:
vector field of spin magnetization
$\vec{m}(\vec{r}, t)$

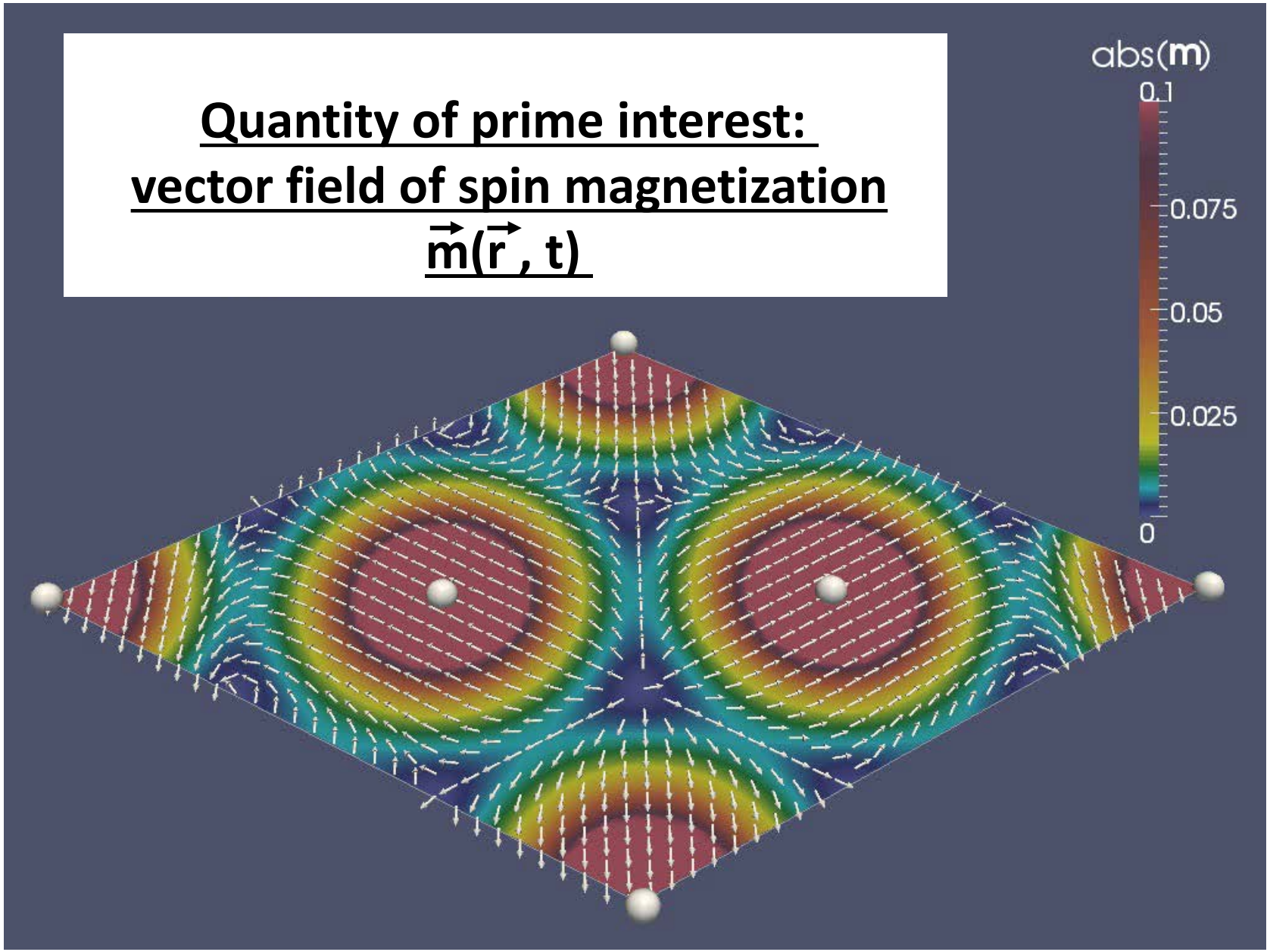

Cr monolayer in ground state

Theoretical Approach: Real-time non-collinear-spin TDDFT with TD spin-orbit coupling

$$i\frac{\partial}{\partial t}\psi_k(r,t)=\Big[\frac{1}{2}\big(-i\nabla-A_{laser}(t)\big)^2+v_S[\rho,\boldsymbol{m}](r,t)-\mu_B\sigma\cdot B_S[\rho,\boldsymbol{m}](r,t)$$
$$+\frac{\mu_B}{2c}\sigma\cdot\big(\nabla v_S[\rho,\boldsymbol{m}](r,t)\big)\times\big(-i\nabla\big)\Big]\psi_k(r,t)$$

$$v_S[\rho,\boldsymbol{m}](r,t)=v_{lattice}(r)+\int\frac{\rho(r',t)}{|r-r'|}d^3r'+v_{xc}[\rho,\boldsymbol{m}](r,t)$$

$$B_S[\rho,\boldsymbol{m}](r,t)=B_{external}(r,t)+B_{xc}[\rho,\boldsymbol{m}](r,t)$$

where $\psi_k(r,t)$ are Pauli spinors

Theoretical Approach: Real-time non-collinear-spin TDDFT with TD spin-orbit coupling

$$i\frac{\partial}{\partial t}\psi_k(r,t)=\left[\frac{1}{2}\left(-i\nabla-A_{laser}(t)\right)^2+v_S[\rho,\boldsymbol{m}](r,t)-\mu_B\sigma\cdot B_S[\rho,\boldsymbol{m}](r,t)\right.$$
$$\left.+\frac{\mu_B}{2c}\sigma\cdot\left(\nabla v_S[\rho,\boldsymbol{m}](r,t)\right)\times\left(-i\nabla\right)\right]\psi_k(r,t)$$

$$v_S[\rho,\boldsymbol{m}](r,t)=v_{lattice}(r)+\int\frac{\rho(r',t)}{|r-r'|}d^3r'+v_{xc}[\rho,\boldsymbol{m}](r,t)$$

$$B_S[\rho,\boldsymbol{m}](r,t)=B_{external}(r,t)+B_{xc}[\rho,\boldsymbol{m}](r,t)$$

Universal functionals of ρ and m

where $\psi_k(r,t)$ are Pauli spinors

$$n(\boldsymbol{r},t)=\sum_{j=1}^{N}\psi_j^{\dagger}(\boldsymbol{r},t)\,\psi_j(\boldsymbol{r},t)$$

$$\vec{\mathbf{m}}(\boldsymbol{r},t)=\sum_{j=1}^{N}\psi_j^{\dagger}(\boldsymbol{r},t)\,\vec{\boldsymbol{\sigma}}\,\psi_j(\boldsymbol{r},t)$$

Aspects of the implementation

- Wave length of laser in the visible regime
  (very large compared to unit cell)

  ⇨ Dipole approximation is made
  (i.e. electric field of laser is assumed to be spatially constant)

  ⇨ Laser can be described by a purely time-dependent vector potential

- **Periodicity of the TDKS Hamiltonian is preserved!**

- **Implementation in ELK code (FLAPW) (http://elk.sourceforge.net/)**

Aspects of the implementation

- Wave length of laser in the visible regime
  (very large compared to unit cell)

  ⇨ Dipole approximation is made
  (i.e. electric field of laser is assumed to be spatially constant)

  ⇨ Laser can be described by a purely time-dependent vector potential

- **Periodicity of the TDKS Hamiltonian is preserved!**

- **Implementation in ELK code (FLAPW) (http://elk.sourceforge.net/)**

Kay Dewhurst

ELK = Electrons in K-Space
or
Electrons in Kay's Space

Sangeeta Sharma

Aspects of the implementation

- Wave length of laser in the visible regime
  (very large compared to unit cell)

  ⇨ Dipole approximation is made
  (i.e. electric field of laser is assumed to be spatially constant)

  ⇨ Laser can be described by a purely time-dependent vector potential

- **Periodicity of the TDKS Hamiltonian is preserved!**

- **Implementation in ELK code (FLAPW) (http://elk.sourceforge.net/)**

Demagnetisation in Fe, Co and Ni

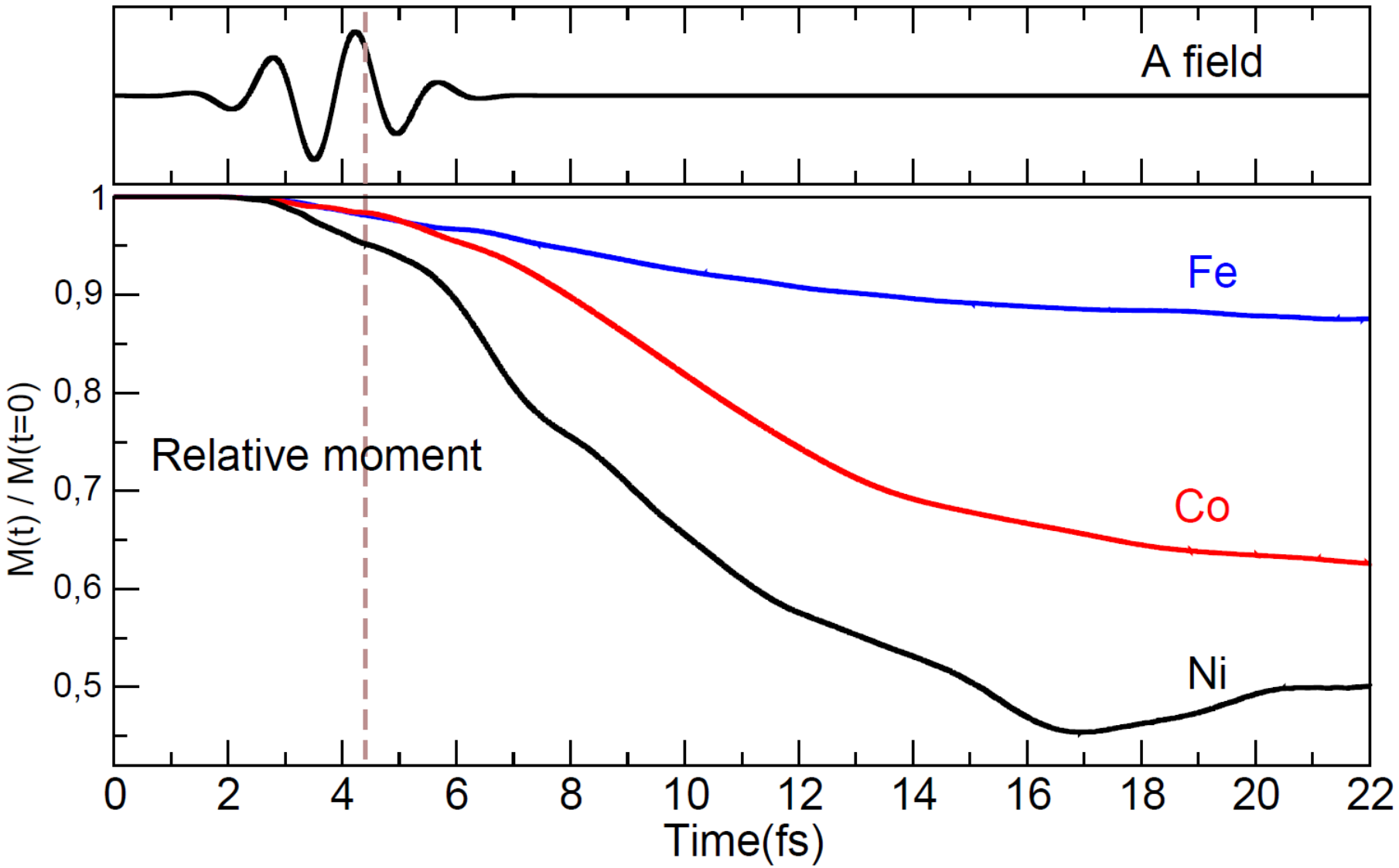

K. Krieger, K. Dewhurst, P. Elliott, S. Sharma, E.K.U.G., JCTC 11, 4870 (2015)

Analysis of the results

Calculation without spin-orbit coupling

components of spin moment

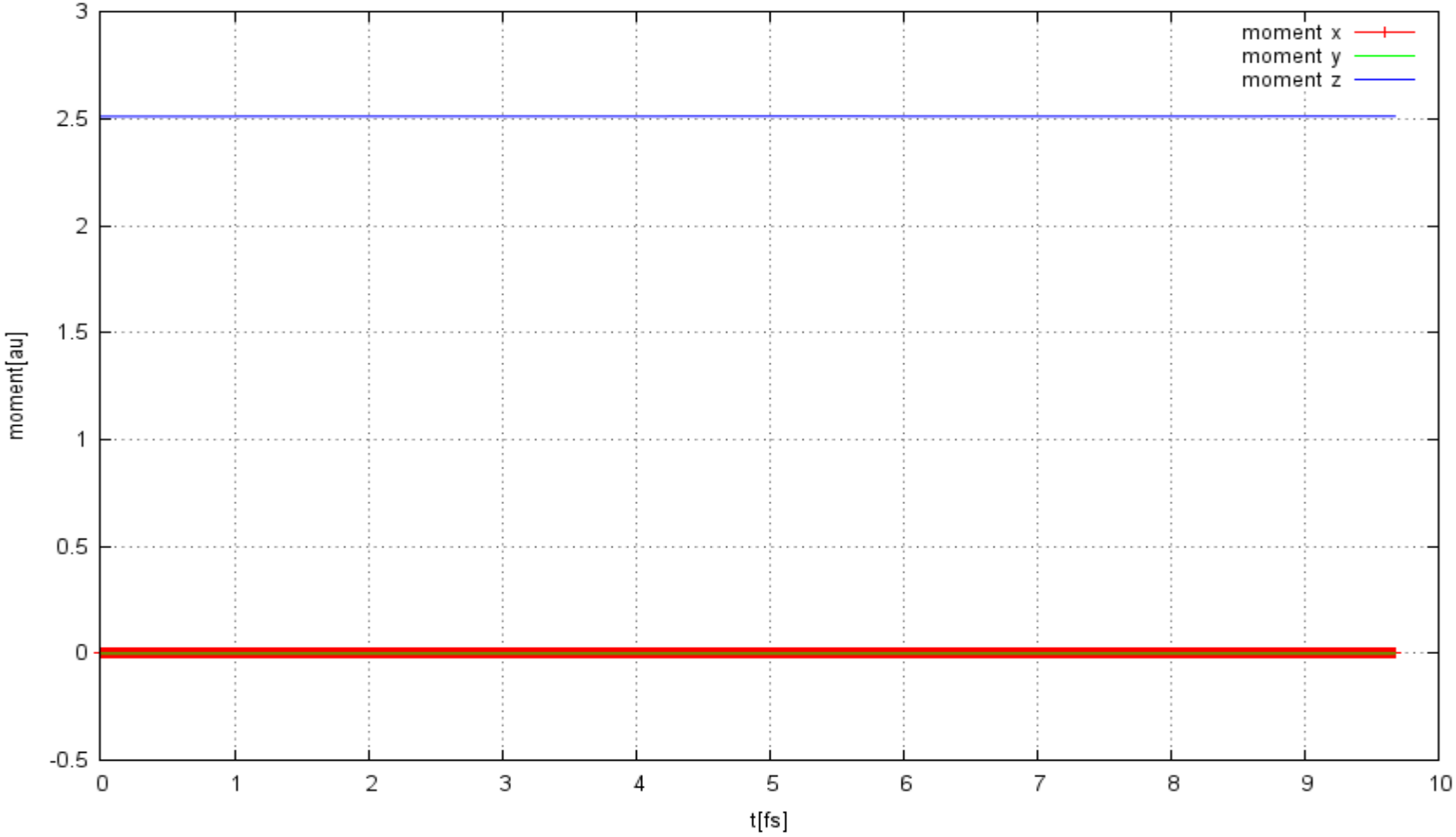

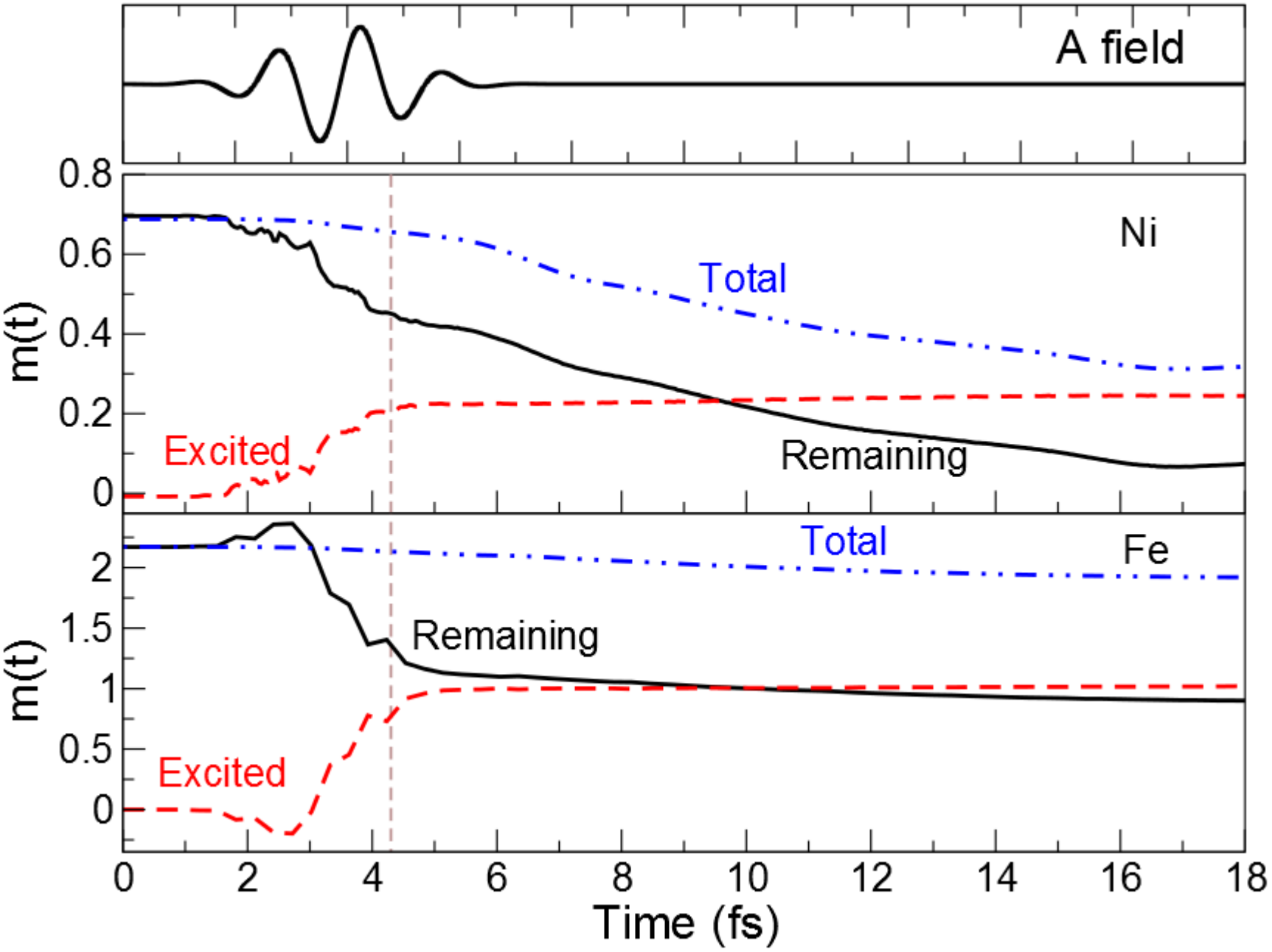
A field
Ni
Total
Excited
Remaining
m(t)
Fe
Total
Remaining
Excited
m(t)
Time (fs)

Demagnetization occurs in two steps:

- Initial excitation by laser *moves* magnetization from atomic region into interstitial region. Total Moment is basically conserved during this phase.

- Spin-Orbit term drives demagnetization of the more localized electrons until stabilization at lower moment is achieved

- This is a local mechanism, hence occurs in this form in essentially all systems, e.g. magnetic clusters (Sanvito group, Dublin) or magnetic mono-layer / few-layer systems

- **K. Krieger, J.K. Dewhurst, P. Elliott, S. Sharma, E.K.U. Gross, JCTC 11, 4870 (2015).**
- **K. Krieger, P. Elliott, T. Müller, N. Singh, J. K. Dewhurst, E.K.U. Gross, S. Sharma, J. Phys. Cond. Matter 29, 224001 (2017).**
- **V. Shokeen, M. Sanchez Piaia, J.Y. Bigot, T. Mueller, P. Elliott, J.K. Dewhurst, S. Sharma, E.K.U. Gross, Phys. Rev. Lett. 119, 107203 (2017).**

Playing with laser parameters

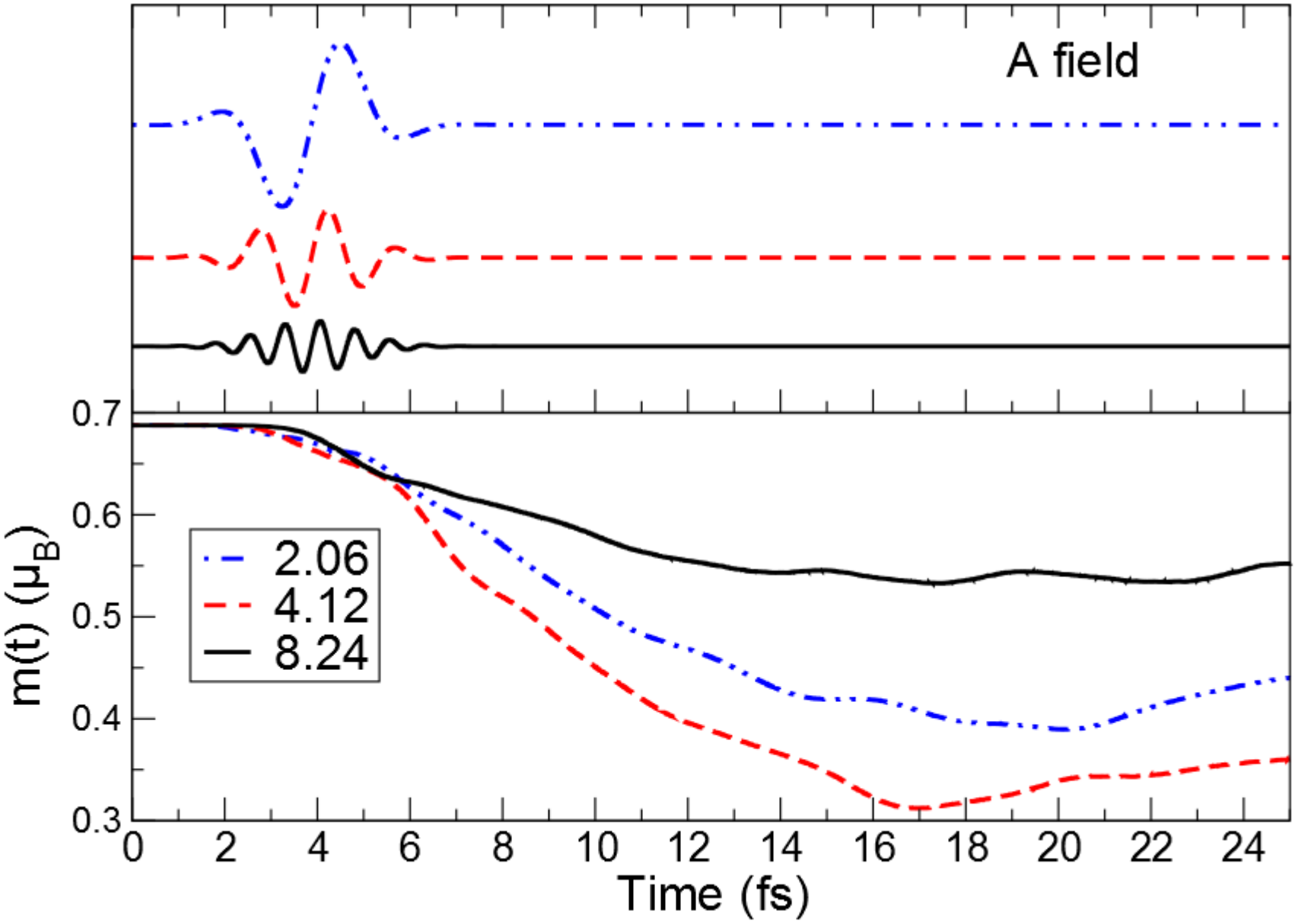
A field
0.7
0.6
0.5
0.4
0.3
m(t) (μB)
2.06
4.12
8.24
0
2
4
6
8
10
12
14
16
18
20
22
24
Time (fs)

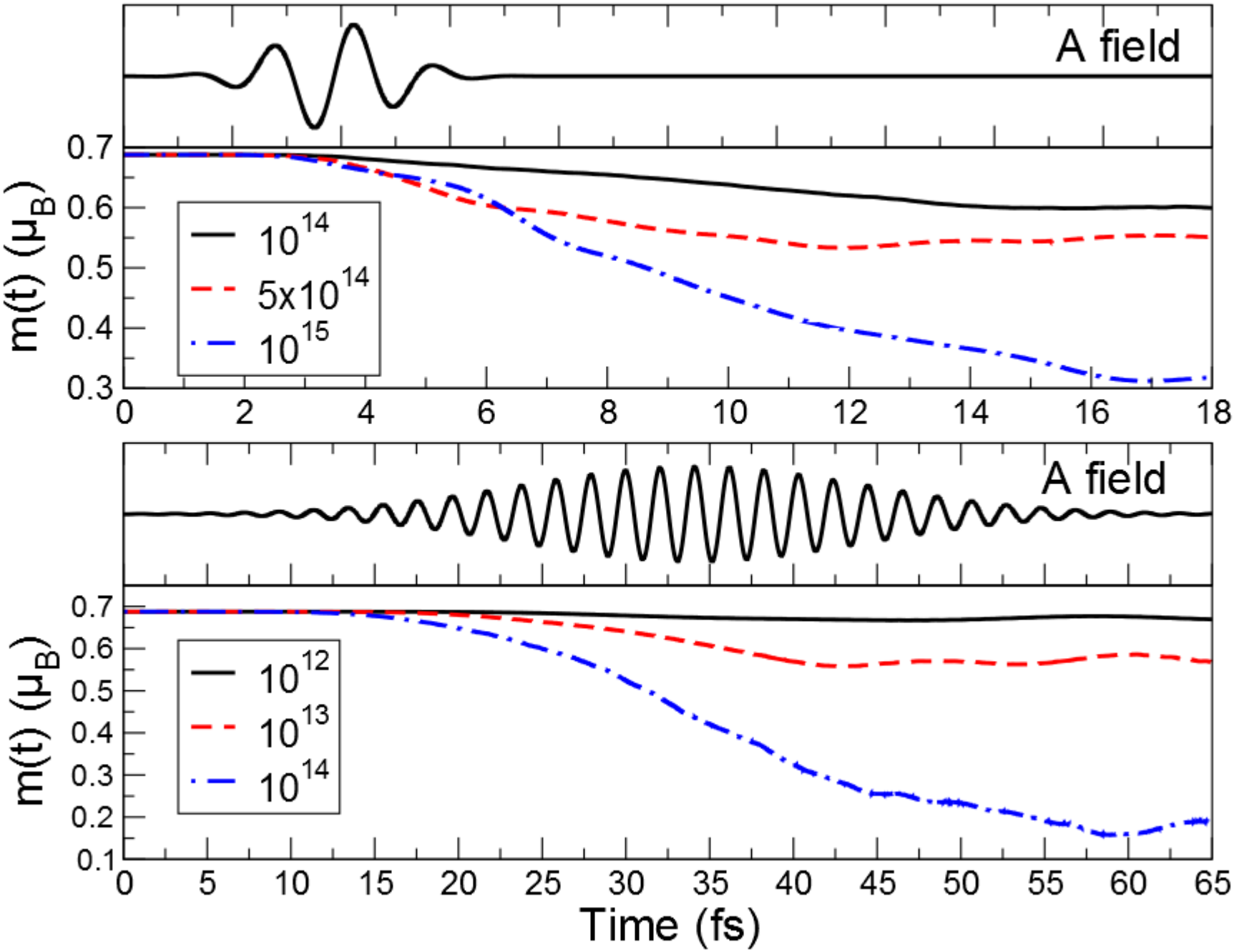
A field
m(t) (μB)
0.7
0.6
0.5
0.4
0.3
10^14
5x10^14
10^15
0
2
4
6
8
10
12
14
16
18
A field
m(t) (μB)
0.7
0.6
0.5
0.4
0.3
0.2
0.1
10^12
10^13
10^14
0
5
10
15
20
25
30
35
40
45
50
55
60
65
Time (fs)

Beyond 3D bulk

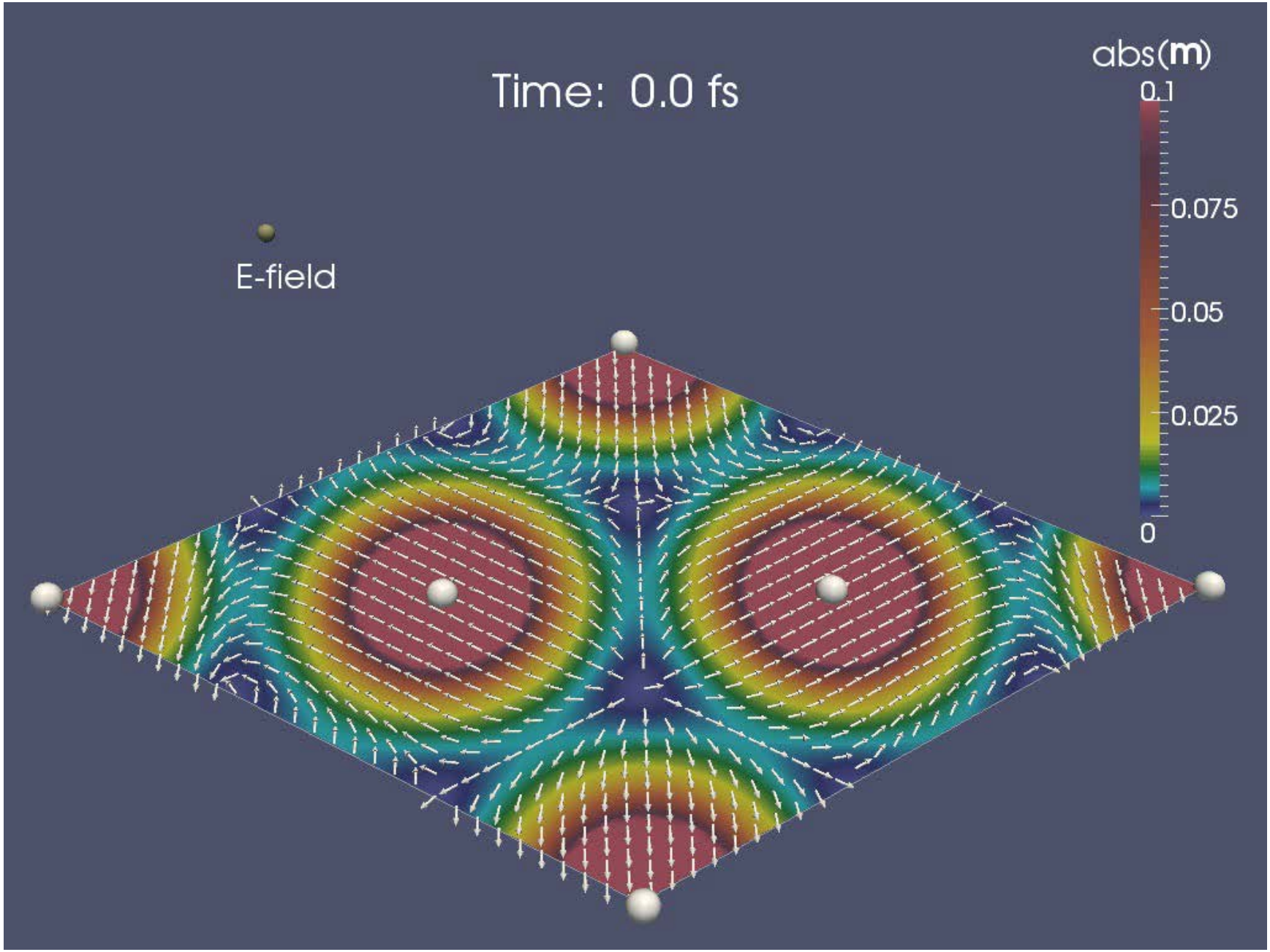

Cr monolayer

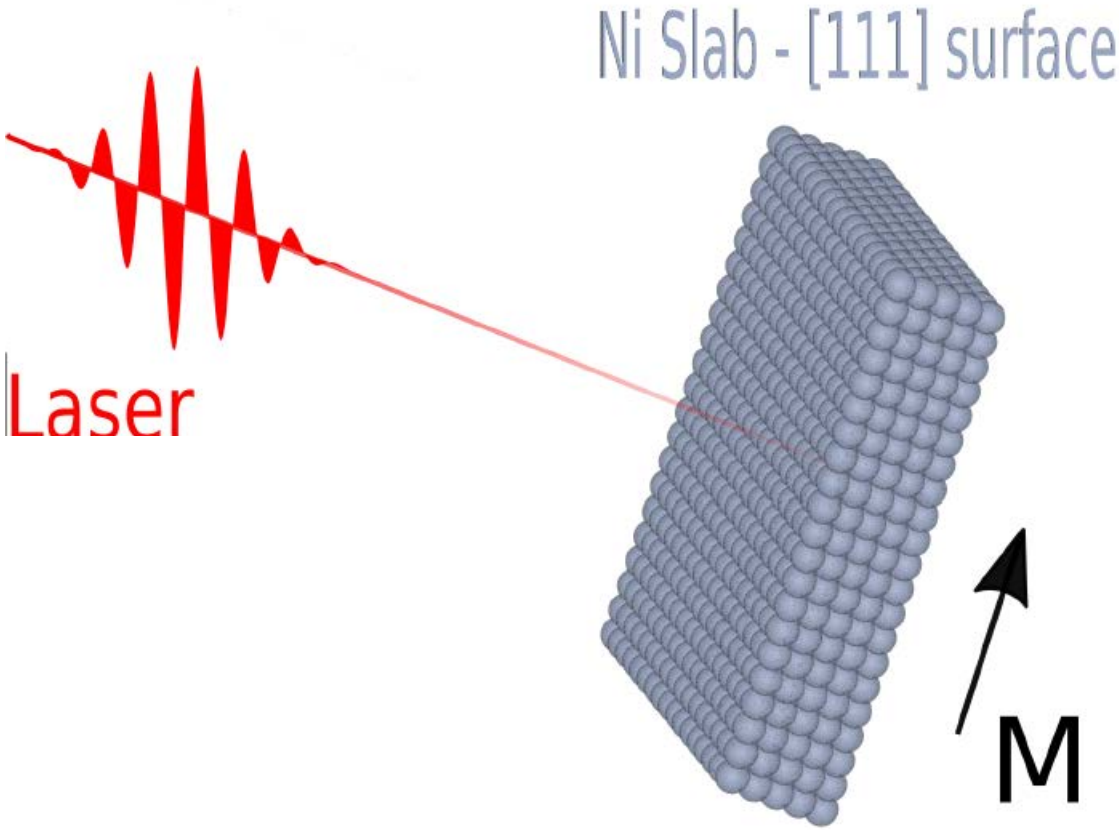
Ni Slab - [111] surface
Laser
M

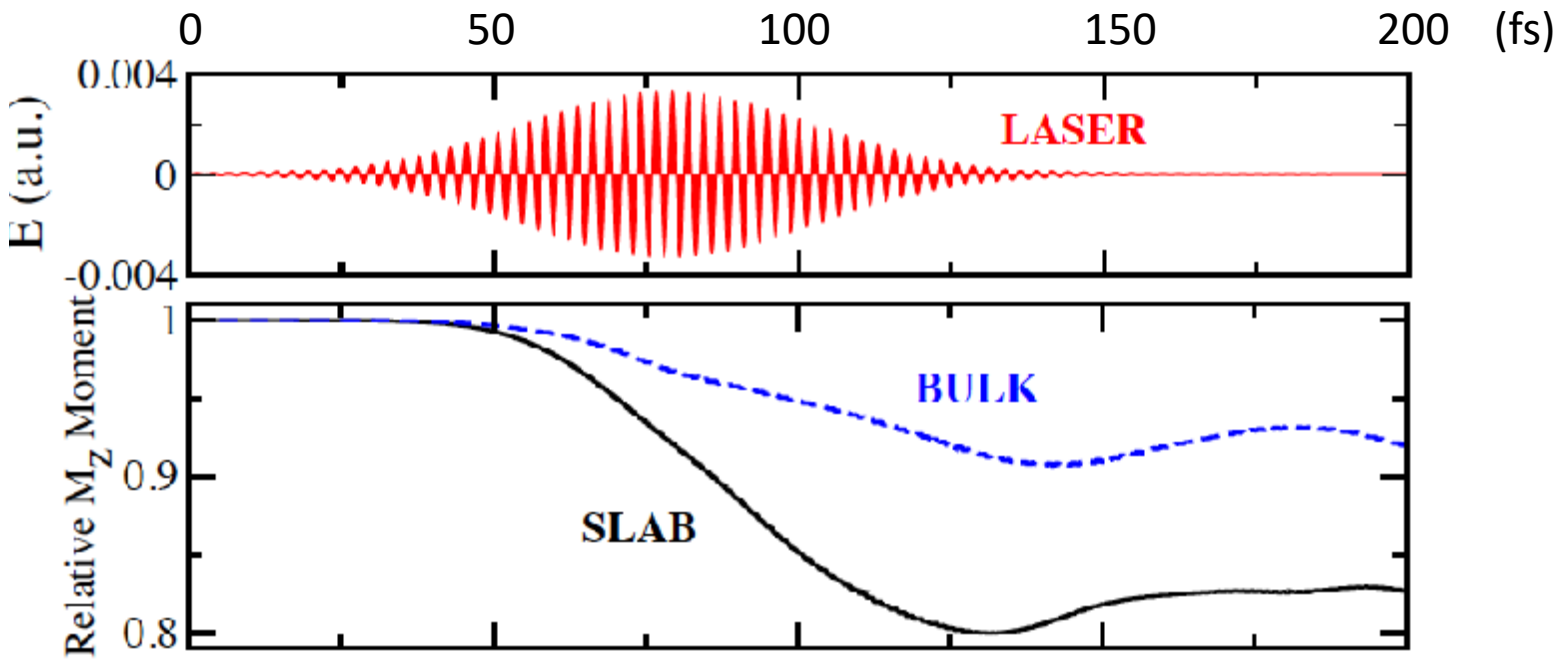
0
50
100
150
200
(fs)
E (a.u.)
0.004
0
-0.004
LASER
Relative M_Z Moment
1
0.9
0.8
BULK
SLAB

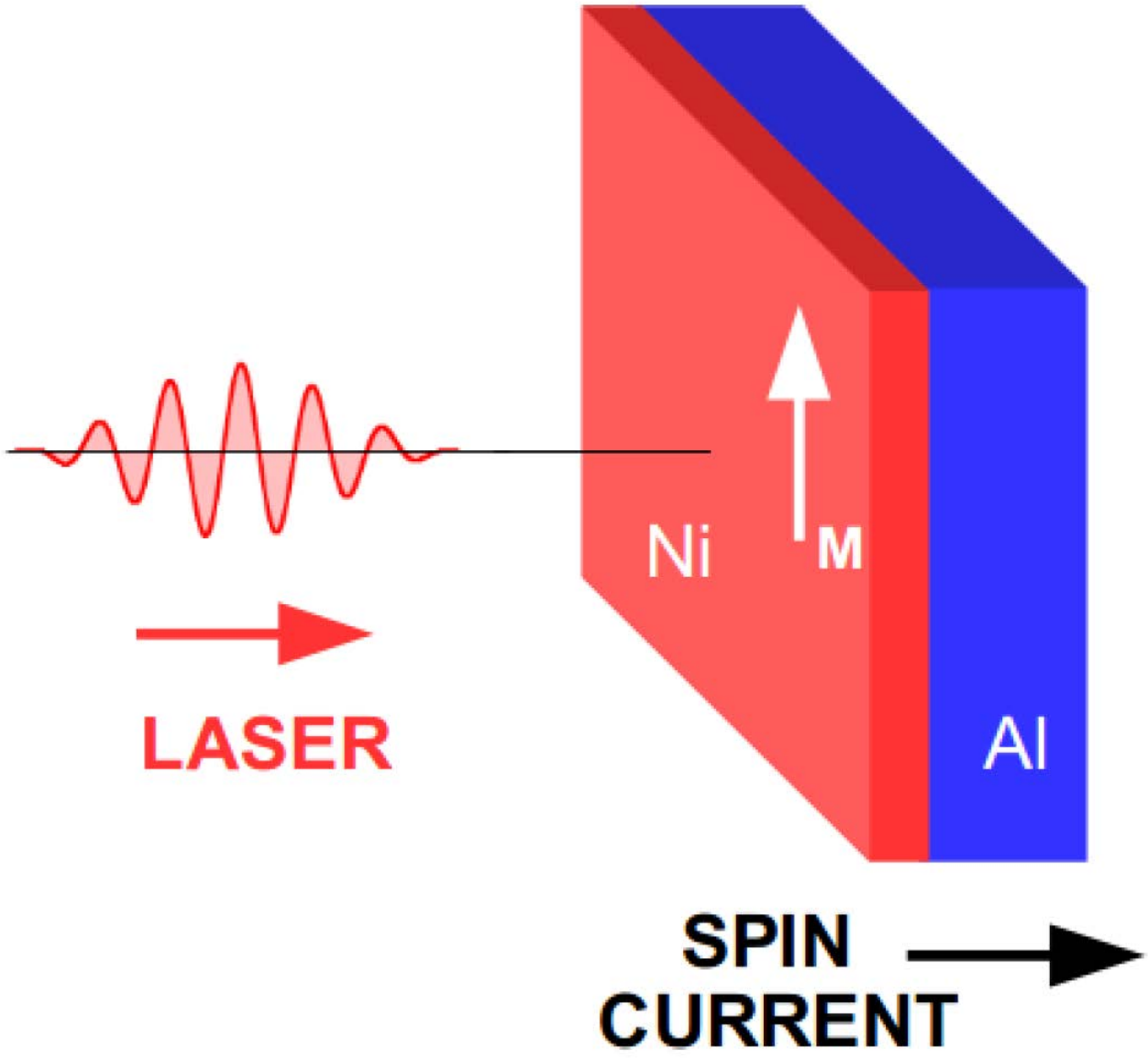
Ni
M
Al
LASER
SPIN
CURRENT

Effect of spin transport across interfaces: Ni@Al

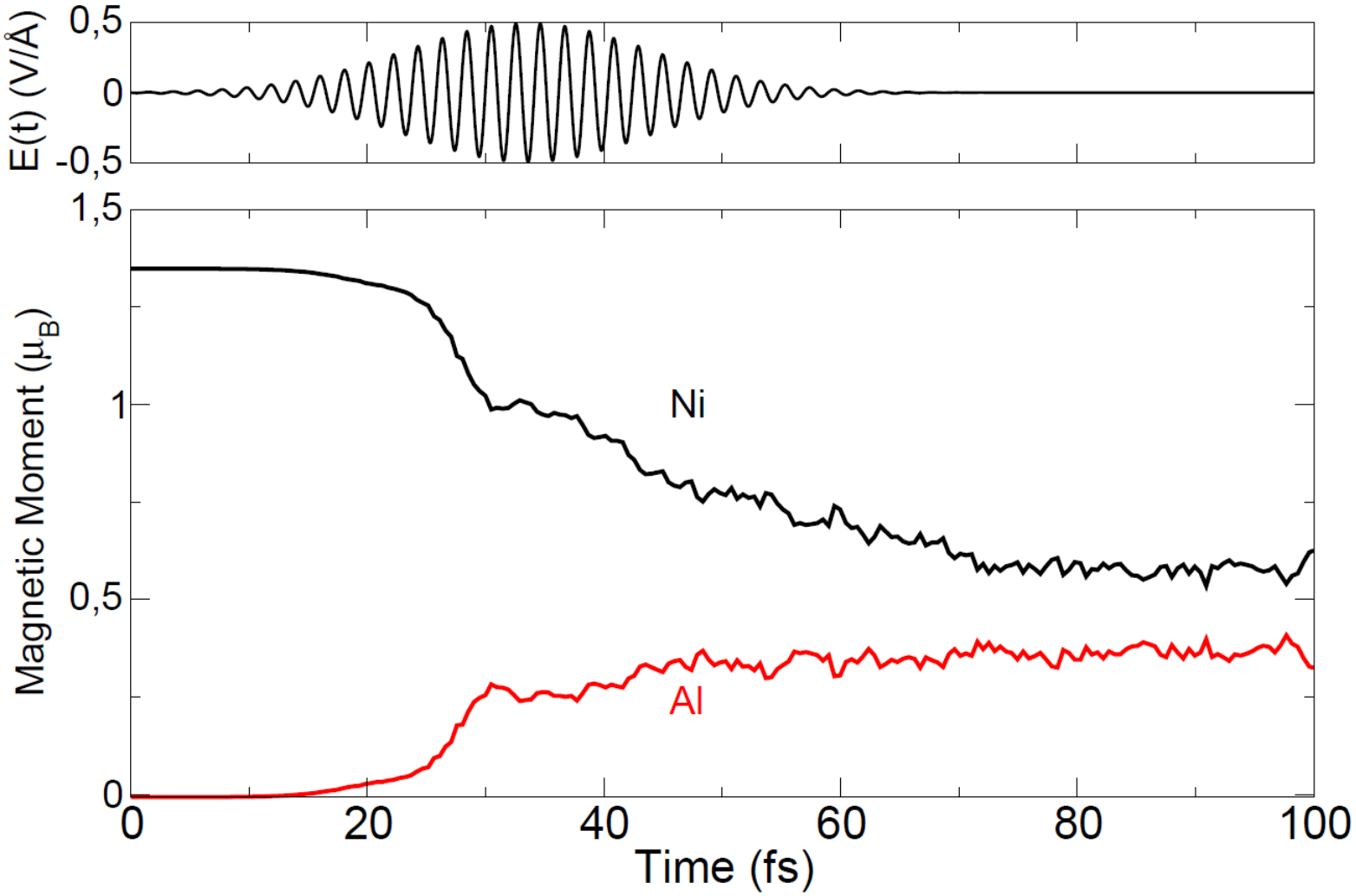

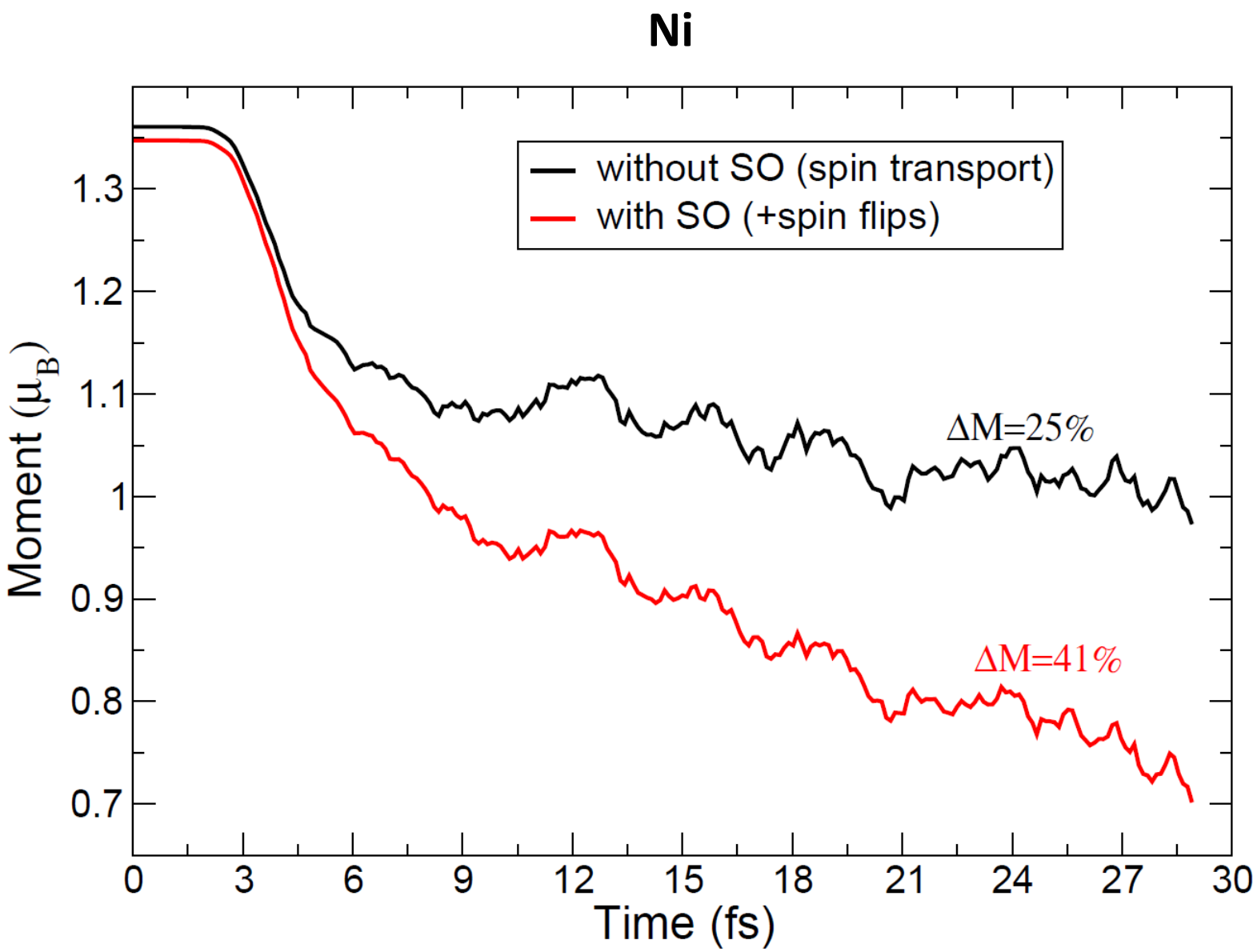
Ni
without SO (spin transport)
with SO (+spin flips)
ΔM=25%
ΔM=41%
Moment (μB)
Time (fs)
0.7
0.8
0.9
1
1.1
1.2
1.3
0
3
6
9
12
15
18
21
24
27
30

Influence of the approximation for the xc functional

Ordinary LSDA yields <u>GLOBAL</u> collinearity

$$\vec{B}_{xc}(r) = \begin{pmatrix} 0 \\ 0 \\ B_{xc}(r) \end{pmatrix} \qquad \vec{m}(r) = \begin{pmatrix} 0 \\ 0 \\ m(r) \end{pmatrix}$$

$\vec{B}_{xc}, \vec{m}$ parallel to $\begin{pmatrix} 0 \\ 0 \\ 1 \end{pmatrix}$ everywhere in space

Construction of non-collinear LSDA

Kübler, Sandratskii (1980s)

$$\int \rho(r) v(r) d^3r - \int \vec{m}(r) \cdot \vec{B}(r) d^3r$$

$$\equiv \sum_{\alpha,\beta=\uparrow\downarrow} \rho_{\alpha,\beta}(r) v_{\alpha,\beta}(r)$$

$\{\rho(r), \vec{m}(r)\}$: 4 independent functions

$\rho_{\alpha\beta}$ is Hermitian $\Rightarrow$ 4 independent functions

Non-collinear LSDA:

$\vec{r}$ given point in space:

① Find unitary matrix U(r) such that

$$U^{+}(r)\left(\rho_{\alpha\beta}\right)U(r)=\begin{pmatrix} n_{\uparrow}(r) & 0 \\ 0 & n_{\downarrow}(r) \end{pmatrix}$$

② Calculate $v_{xc}^{\uparrow}(r)$ and $v_{xc}^{\downarrow}(r)$ from $\{n_{\uparrow}, n_{\downarrow}\}$

using the normal LSDA expressions

③ $$\left(v_{xc}^{\alpha\beta}\right)=U(r)\begin{pmatrix} v_{xc}^{\uparrow}(r) & 0 \\ 0 & v_{xc}^{\downarrow}(r) \end{pmatrix}U^{+}(r)$$

in this approximation $\vec{B}_{xc}(r)$ and $\vec{m}(r)$ may change their direction in space, but locally they are always parallel

Problem: In all standard approximations of E_{xc} (LSDA, GGAs) m(r) and $B_{xc}(r)$ are locally parallel

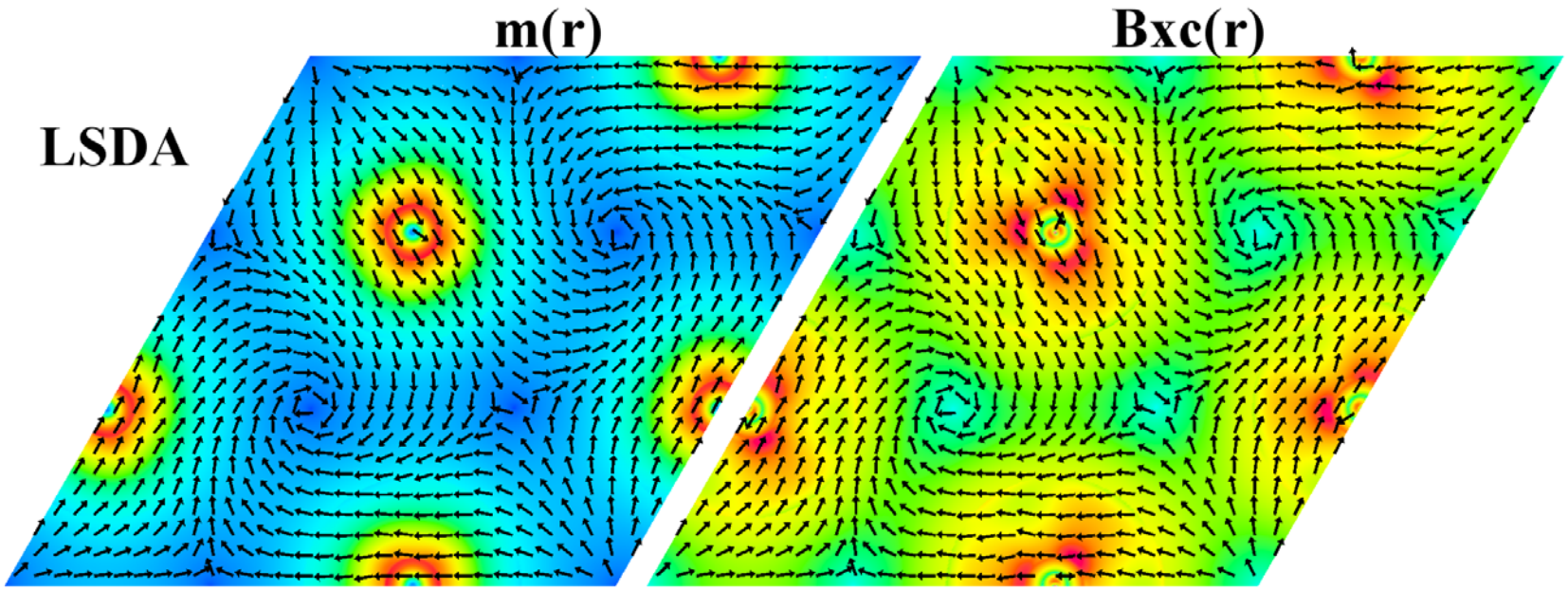

S. Sharma, J.K. Dewhurst, C. Ambrosch-Draxl, S. Kurth, N. Helbig, S. Pittalis, S. Shallcross, L. Nordstroem E.K.U.G., Phys. Rev. Lett. 98, 196405 (2007)

Why is that important?

Ab-initio description of spin dynamics:

microscopic equation of motion (following from TDSDFT)

$$\dot{\vec{m}}(\vec{r},t) = \vec{m}(\vec{r},t)\times\vec{B}_{XC}(\vec{r},t) - \vec{\nabla}\cdot\overleftrightarrow{J}_S(\vec{r},t)+SOC$$

in absence of external magnetic field

$\overleftrightarrow{J}_S(r,t)=\langle\hat{\sigma}\otimes\hat{p}\rangle$ spin current tensor

Consequence of local collinearity: $m\times B_{xc} = 0$:

→ possibly wrong spin dynamics

→ how important is this term in real-time dynamics?

Construction of a novel xc functional for which m(r) and $B_{xc}(r)$ are not locally parallel

Enforce property of the exact xc functional:

$$\boldsymbol{B}_{xc}^{exact}\left(\boldsymbol{r}\right)=\nabla\times A_{xc}^{exact}\left(\boldsymbol{r}\right)$$

K. Capelle, E.K.U. Gross, PRL 78, 1872 (1997)

By virtue of Helmholtz' theorem, any vector field can be decomposed as:

$$\boldsymbol{B}_{xc}^{GGA}\left(\boldsymbol{r}\right)=\nabla\times A_{xc}\left(\boldsymbol{r}\right)+\nabla\phi(r)$$

Enforce exact property by subtracting source term!

Explicit construction:

S. Sharma, E.K.U. Gross, A. Sanna, K. Dewhurst, JCTC14, 1247 (2018)

$$\nabla^2 \phi(\boldsymbol{r}) = 4\pi \nabla \cdot B_{xc}^{GGA}(\boldsymbol{r})$$

$$\tilde{B}_{xc}(\boldsymbol{r}) \cong B_{xc}^{GGA}(\boldsymbol{r}) - \frac{1}{4\pi} \nabla \phi(\boldsymbol{r})$$

$$B_{xc}^{SF}(\boldsymbol{r}) = s\, \tilde{B}_{xc}(\boldsymbol{r})$$

Scaling factor, s, only depends on underlying functional (GGA/LSDA), nothing else

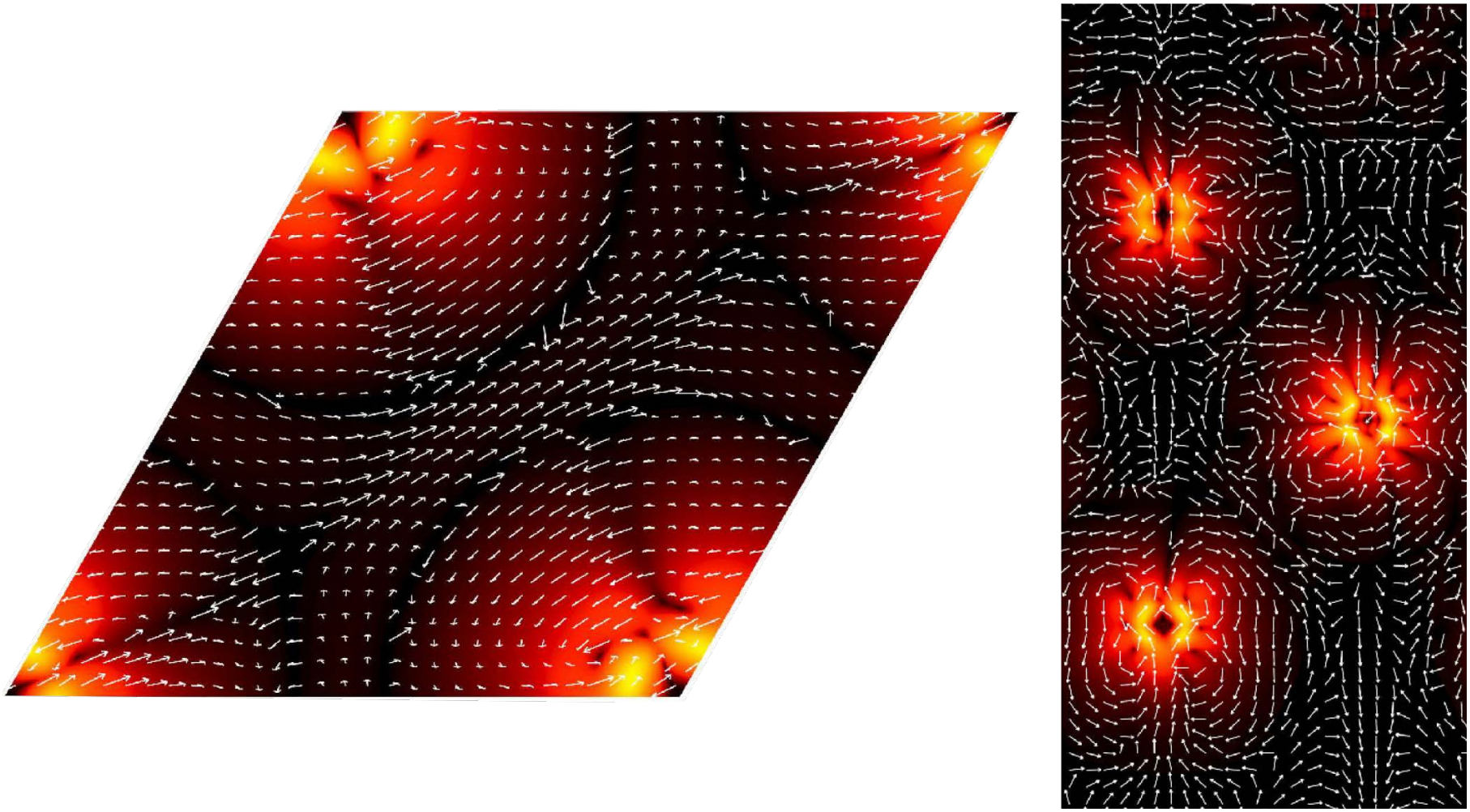

Left panel: Local xc torque for bulk Ni in (111) plane. Right panel: Local xc torque for 3ML Ni@5ML Pt in the (110) plane. The arrows indicate the direction and colors the magnitude.

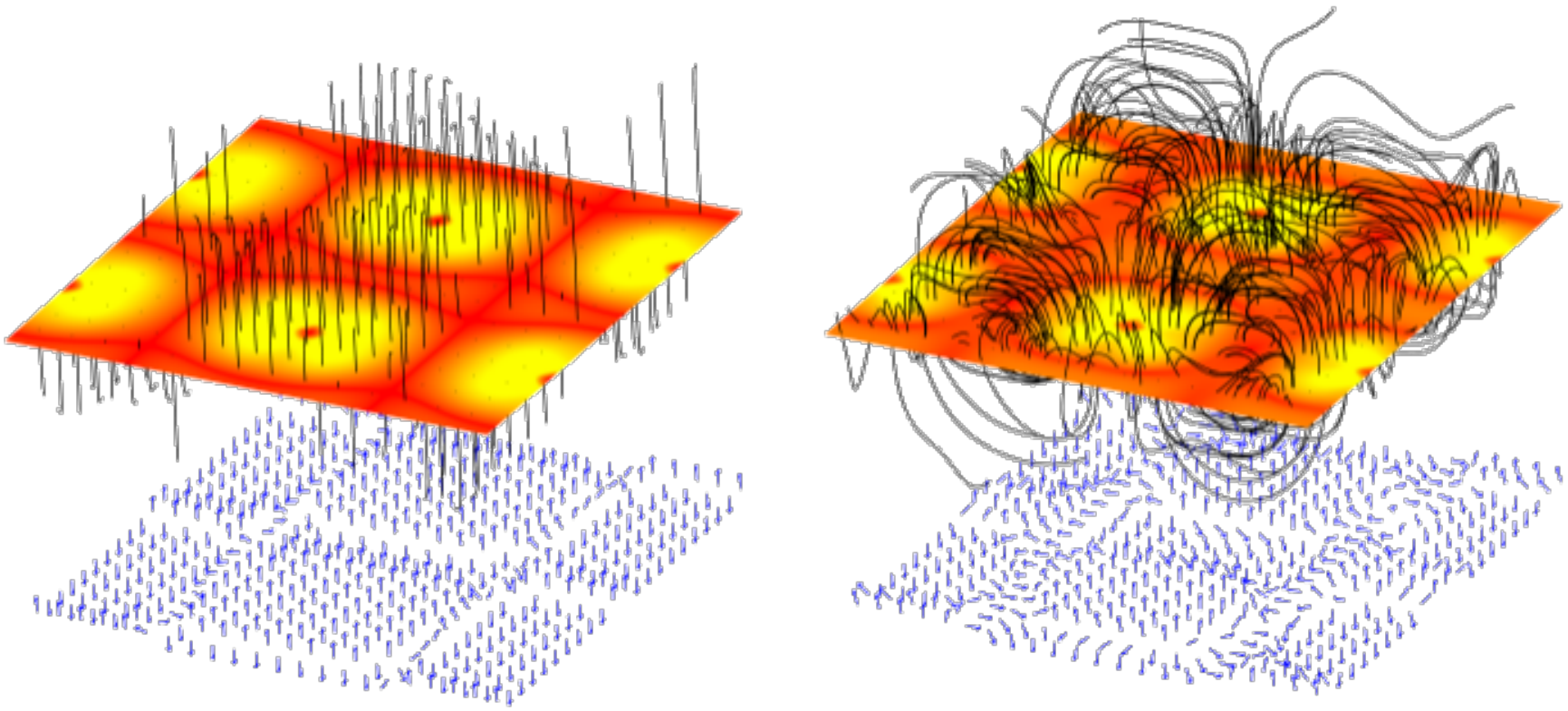

The vector field B_{xc} for $BaFe_2As_2$ projected in a plane containing Fe atoms. Plot (a) is LSDA and plot (b) is source-free LSDA. The colored plane shows the magnitude of B_{xc} and the arrows indicate the direction. The black field lines originate from a regular grid in the plane and follow the vector field. LSDA field lines show a plane of magnetic monopoles while making LSDA source-free leads to more complicated but physical field lines. The arrows indicate that the removal of the source term leads to enhancement of non-collinearity.

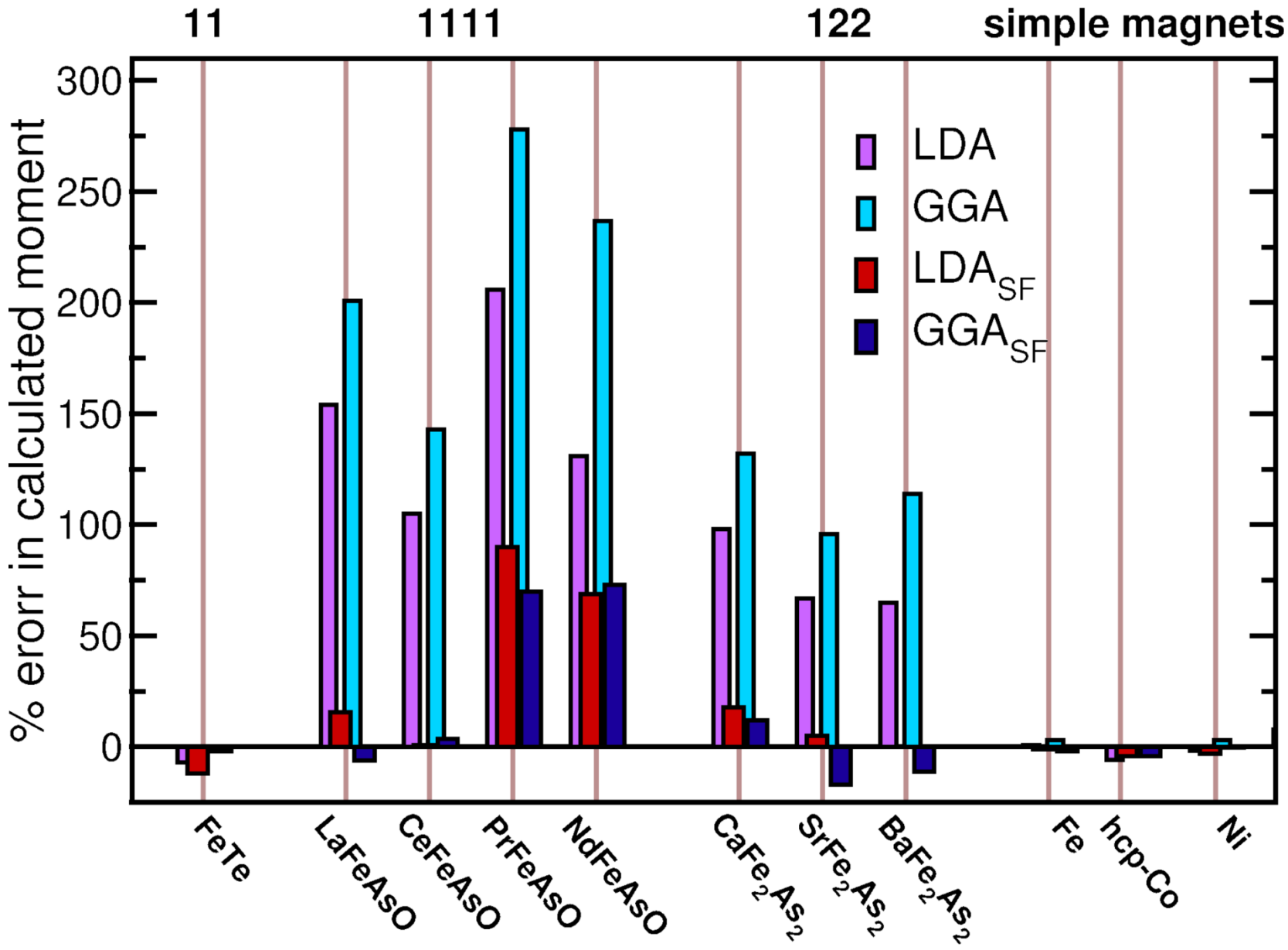
11
1111
122
simple magnets
% erorr in calculated moment
300
250
200
150
100
50
0
LDA
GGA
LDA$_{SF}$
GGA$_{SF}$
FeTe
LaFeAsO
CeFeAsO
PrFeAsO
NdFeAsO
CaFe$_2$As$_2$
SrFe$_2$As$_2$
BaFe$_2$As$_2$
Fe
hcp-Co
Ni

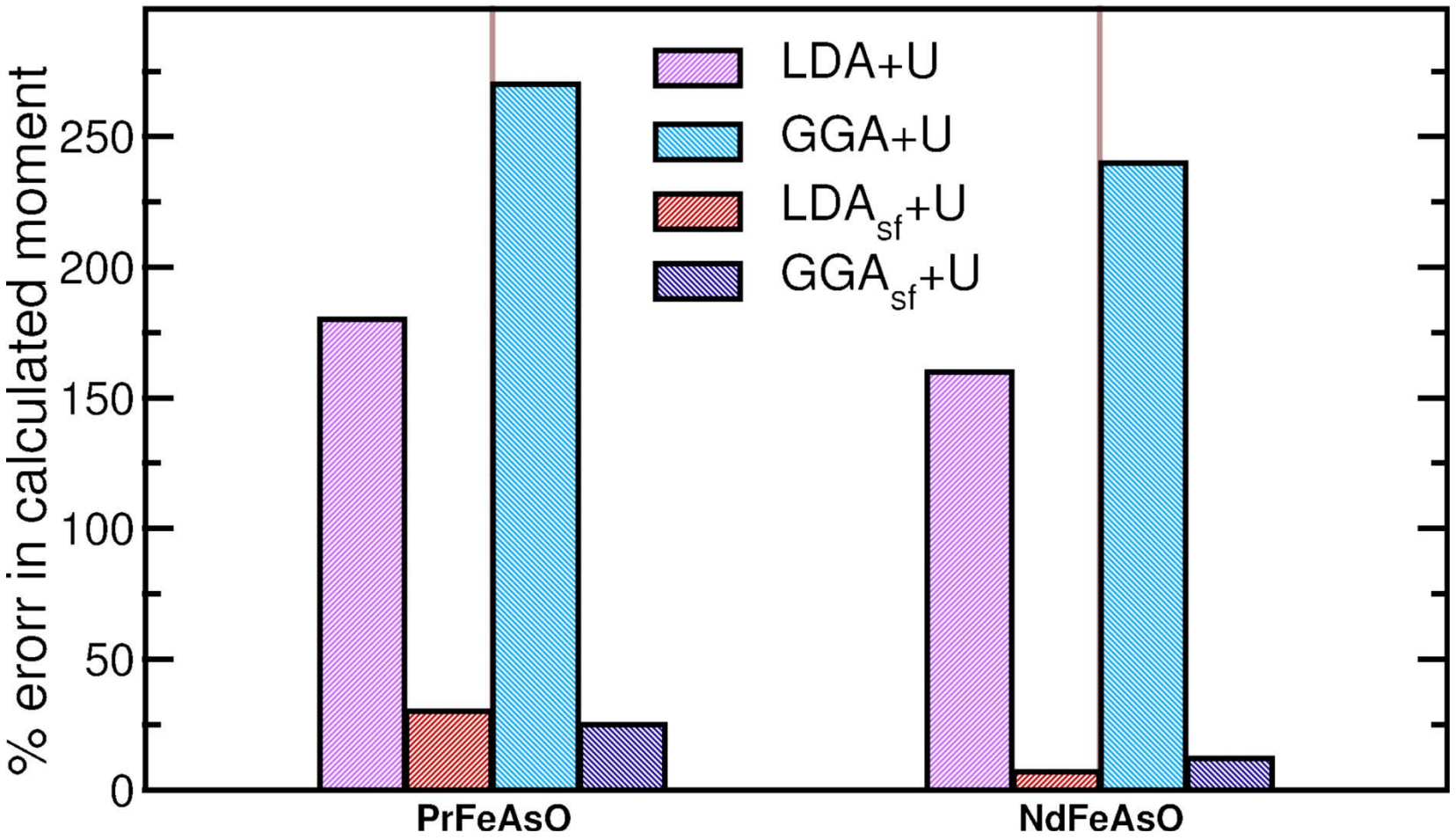
% erorr in calculated moment
0
50
100
150
200
250
LDA+U
GGA+U
LDA$_{sf}$+U
GGA$_{sf}$+U
PrFeAsO
NdFeAsO

Magnetic moment per atom. Calculations are performed using LSDA+U, PBE-GGA+U, $LSDA_{SF}$ + U and PBE-GGA_{SF} + U.

Material	Expt	LSDA	PBE-GGA	$LSDA_{SF}$	PBE-GGA_{SF}
PrFeAsO	Fe: 0.5	1.40	1.9	0.65	0.63
	Pr: 0.87	0.30	0.30	0.81	0.83
NdFeAsO	Fe: 0.54	1.42	1.84	0.50	0.61
	Nd: 0.9	2.44	1.25	0.80	0.89

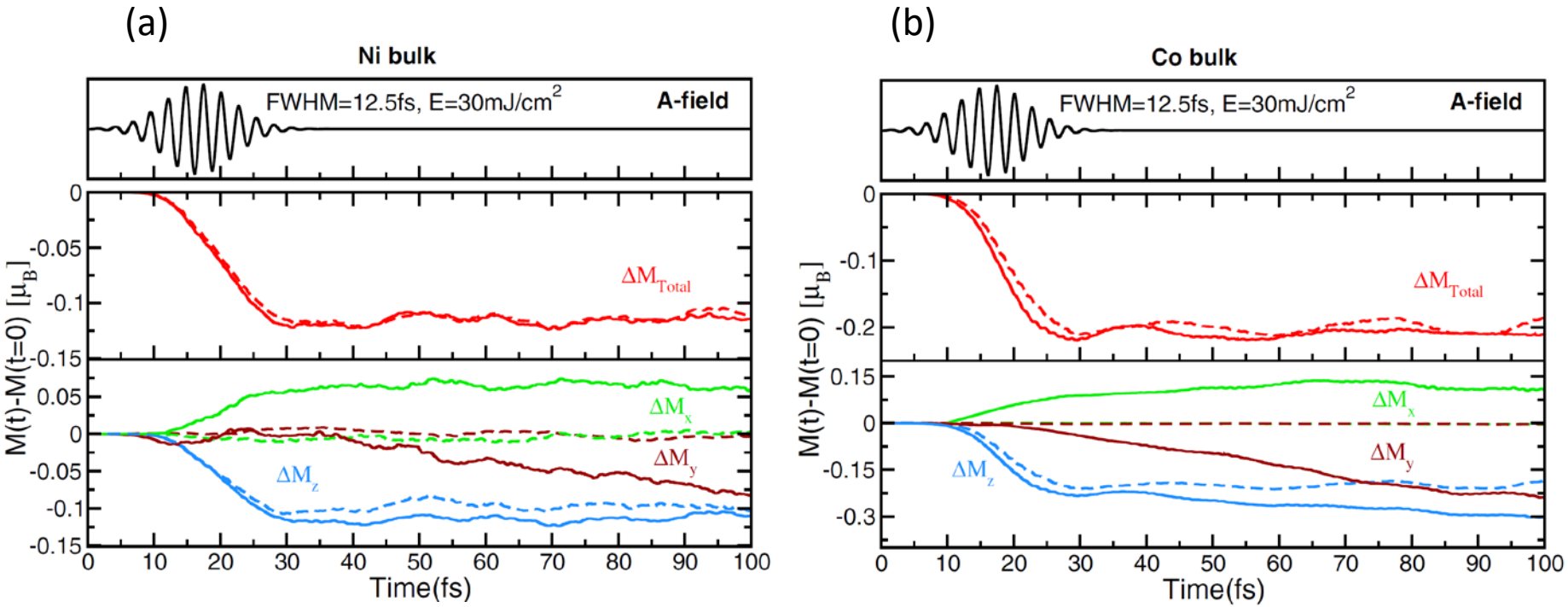

(a) Middle panel shows the total moment (red) and the bottom panel x (green), y (brown) and z (blue) projected moments for bulk Ni as a function of time. Dashed lines are the results obtained using the ALSDA and full lines the results obtained using the source-free functional. (b) The same as (a) but for bulk Co.

Optically induced spin transfer (OISTR)

P. Elliott, T. Mueller, K. Dewhurst, S. Sharma, E.K.U.Gross,
Scientific Reports 6, 38911 (2016)

K. Dewhurst, P. Elliott, S. Shallcross, E.K.U. Gross, S. Sharma,
Nano Lett. 18, 1842 (2018)

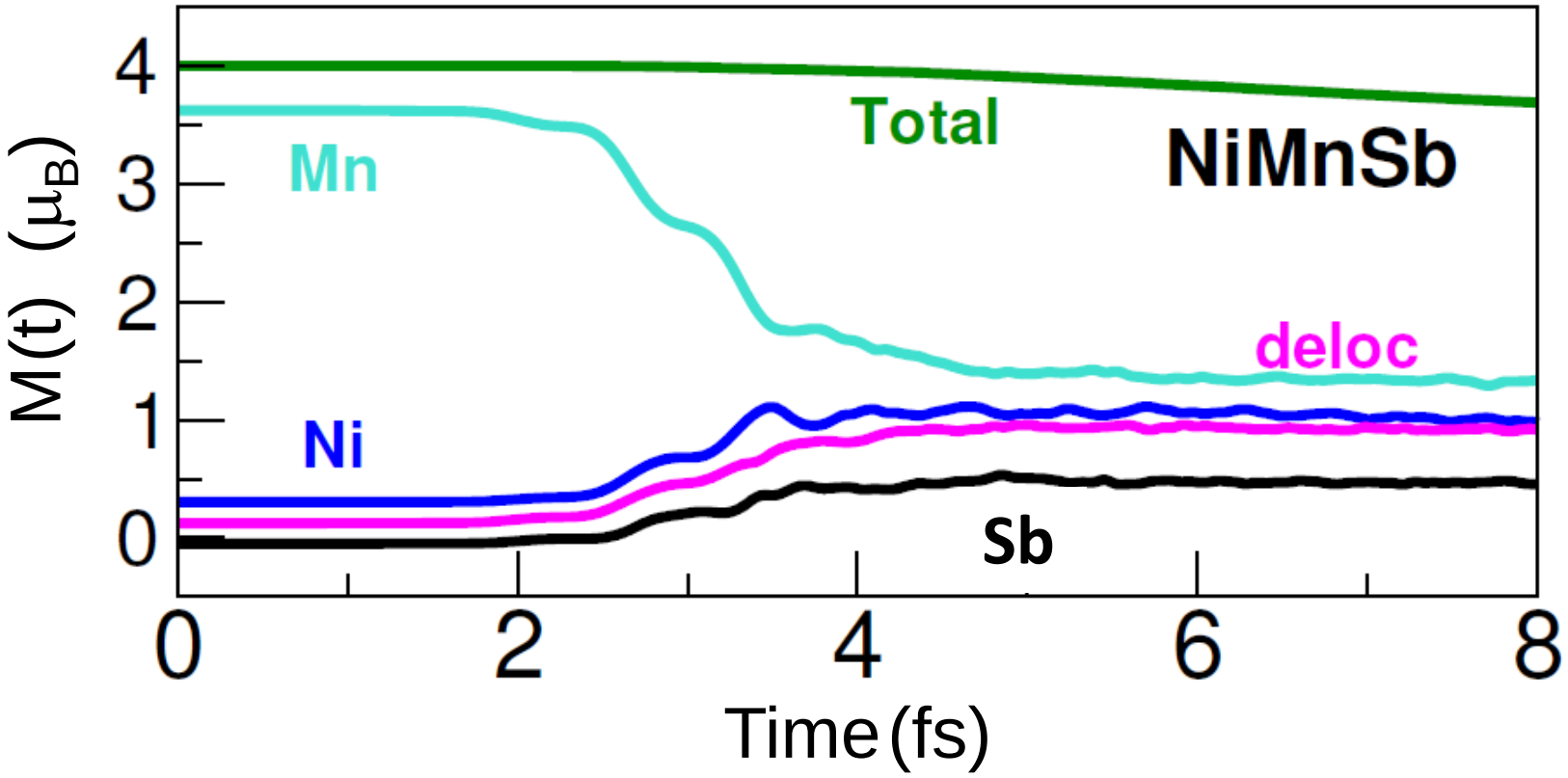

Global moment |M(t)| nearly preserved
Local moments around each atom change

NiMnSb

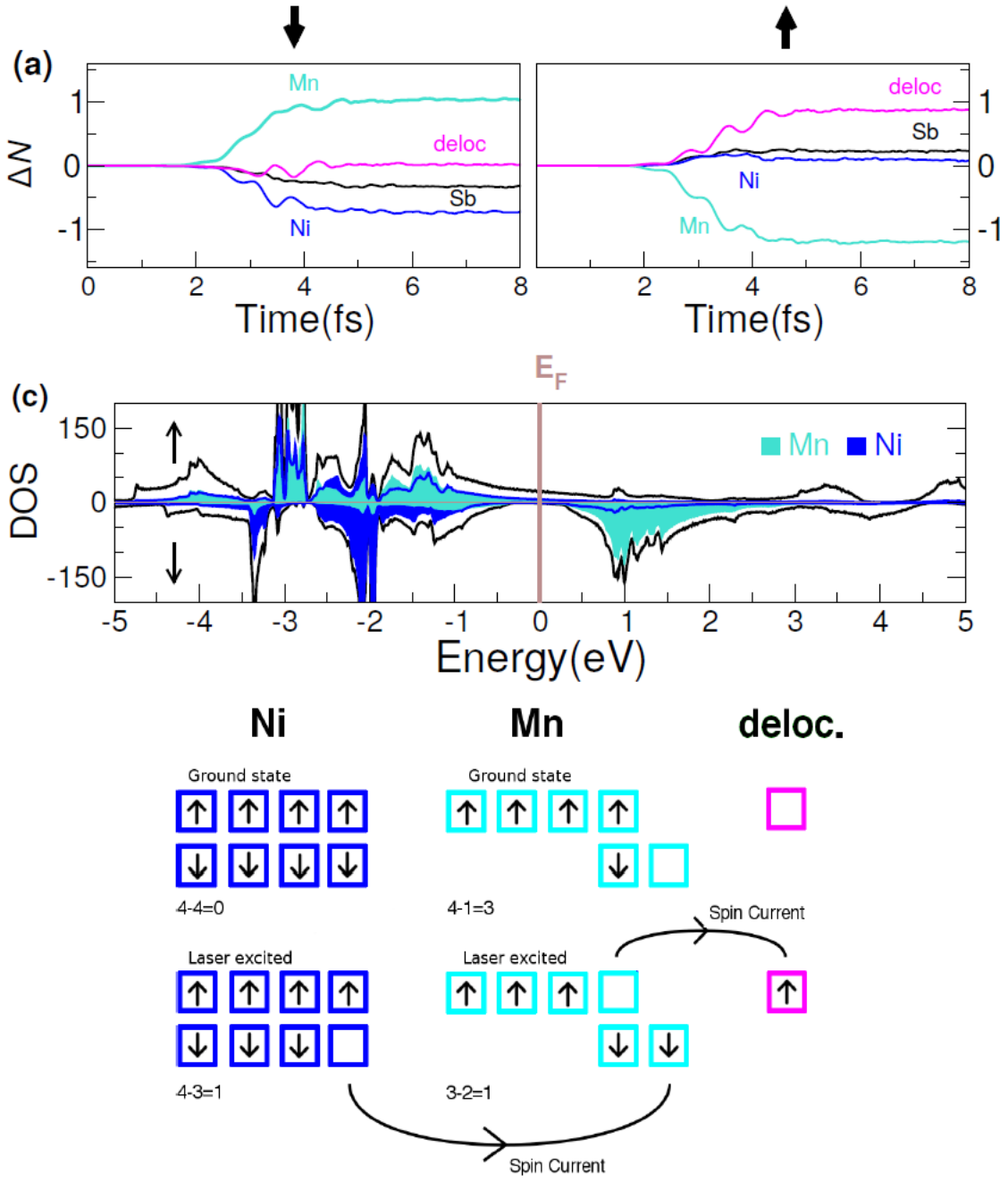
(a)
ΔN
Mn
deloc
Sb
Ni
Time(fs)
deloc
Sb
Ni
Mn
Time(fs)
(c)
DOS
E_F
Mn
Ni
Energy(eV)
Ni
Mn
deloc.
Ground state
4-4=0
Ground state
4-1=3
Spin Current
Laser excited
4-3=1
Laser excited
3-2=1
Spin Current

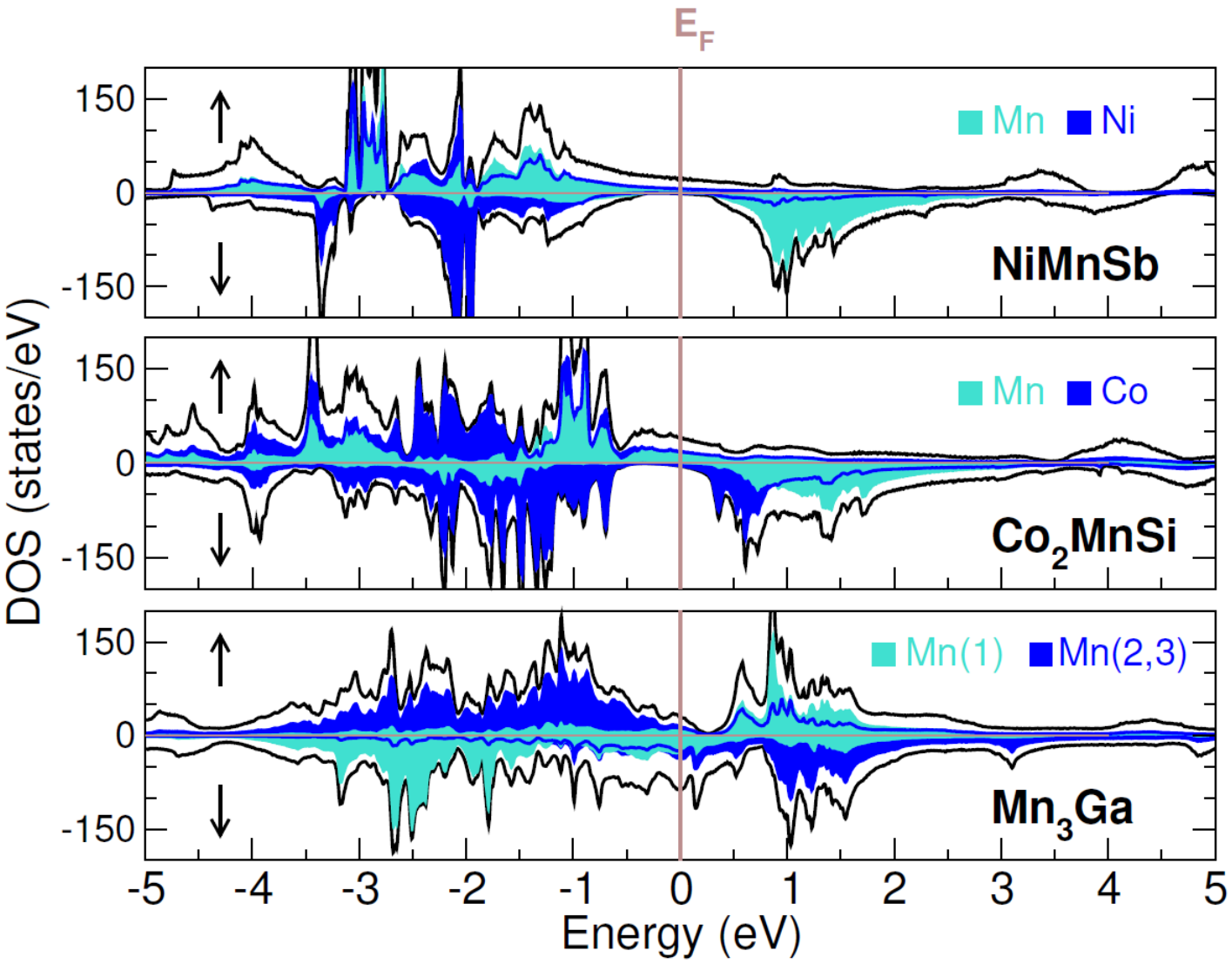
E_F
150
0
-150
Mn
Ni
NiMnSb
Co
Co2MnSi
Mn(1)
Mn(2,3)
Mn3Ga
DOS (states/eV)
-5
-4
-3
-2
-1
0
1
2
3
4
5
Energy (eV)

Mn_3Ga (ferri-magnet)

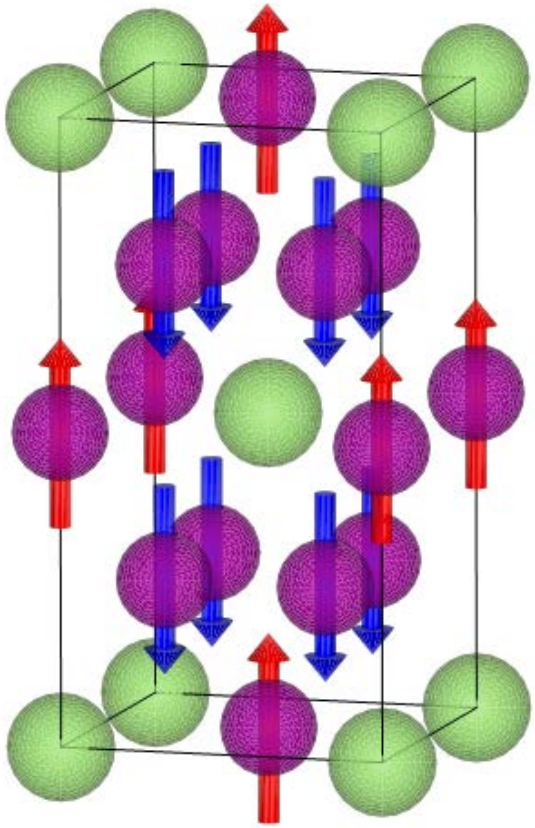

Ga

Mn

TDDFT prediction for Mn_3Ga: ferri → ferro transition within 4 fs

Mn_3Ga (ferri-magnet)

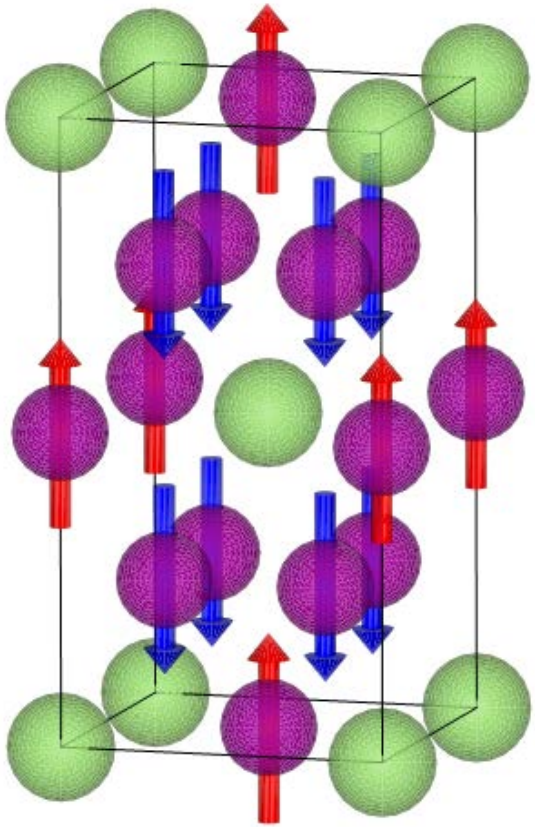

Ga

Mn

TDDFT prediction for Mn_3Ga: ferri → ferro transition within 4 fs

OISTR experimentally confirmed! (Aeschlimann group, 2018)

Coworkers

Kevin Krieger

Sangeeta Sharma

Kay Dewhurst

Peter Elliott

Summary

- Real-time TDDFT implemented in ELK (http://elk.sourceforge.net/)

- Demagnetization in first 50 fs is a **universal** two-step process:
  1. Initial excitation of electrons into highly excited delocalised states (without much of a change in the total magnetization)
  2. Spin-orbit coupling drives demagnetization of the more localized electrons

- Interfaces show spin currents as important as spin-orbit coupling

- New source-free xc functional
  - dramatically improves description of magnetic properties (pnictides)
  - non-vanishing local xc torque changes spin dynamics slightly

- OISTR: Ultrafast (5 fs) transfer of spin moment between sublattices. TDDFT prediction experimentally cofirmed

Future aspects in the field of laser-driven spin dynamics:

- **Include relaxation processes due to el-el scattering**
  - in principle contained in TDDFT,
  - but not with adiabatic xc functionals
  - need xc functional approximations with memory $v_{xc}\left[\rho(r't')\right](rt)$

- **Include relaxation processes due to el-phonon scattering**

- **Include relaxation due to radiative effects**
  simultaneous propagation of TDKS and Maxwell equations

- **Include dipole-dipole interaction to describe motion of domains**
  construct approximate xc functionals which refer to the dipole int

- **Optimal-control theory to find optimized laser pulses**
  to selectively demagnetize/remagnetize, i.e. to switch,
  the magnetic moment
- **Create Skyrmions with suitably shaped laser pulses**

Electronic transport with TDDFT

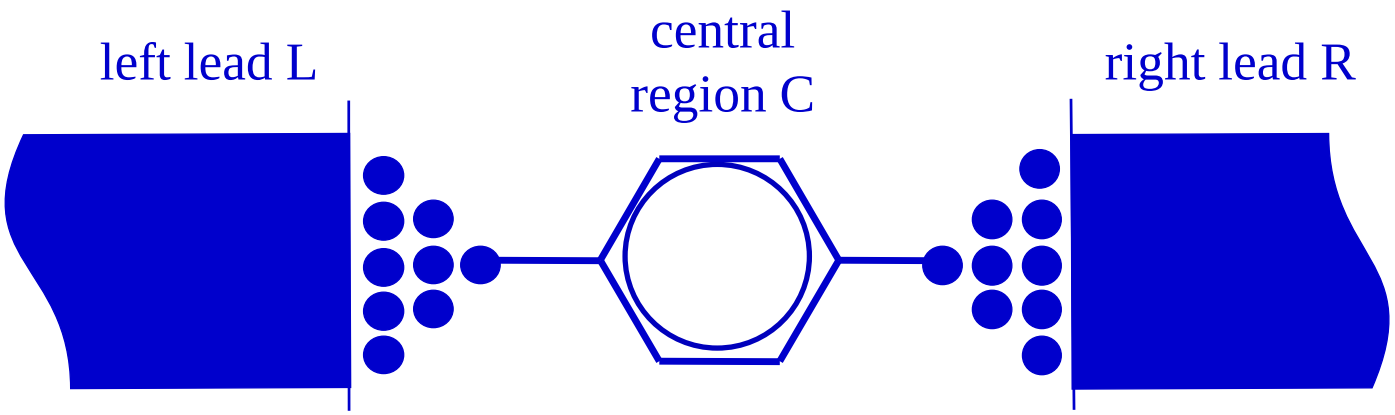

Bias between L and R is turned on: U(t) $\longrightarrow$ V for large t

Electronic transport with TDDFT

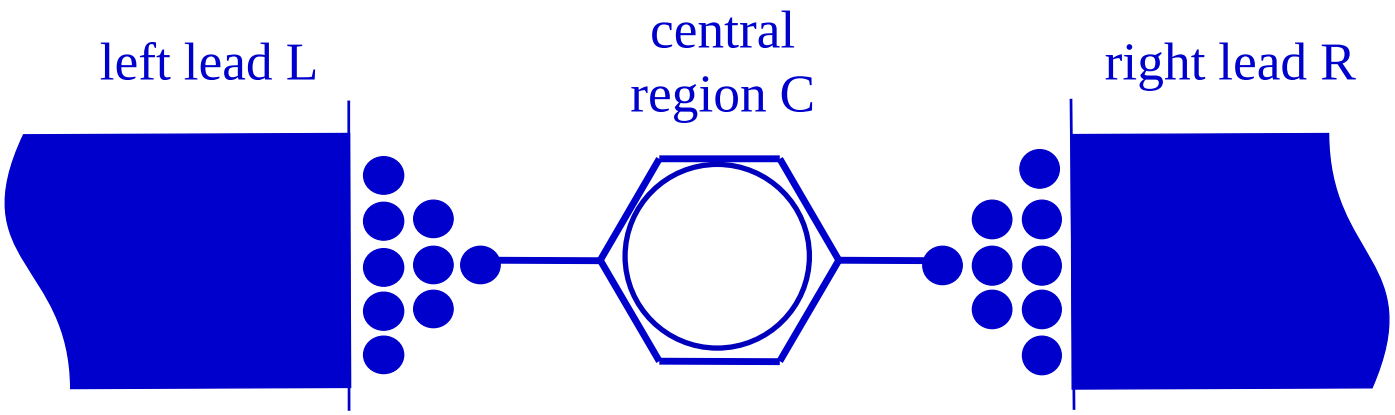

Bias between L and R is turned on: U(t) $\longrightarrow$ V for large t

Questions:

- After switching-on, does one always reach a steady state?
- Is the steady state unique?
- How to deal with time-dependent external fields?

Electronic transport with TDDFT

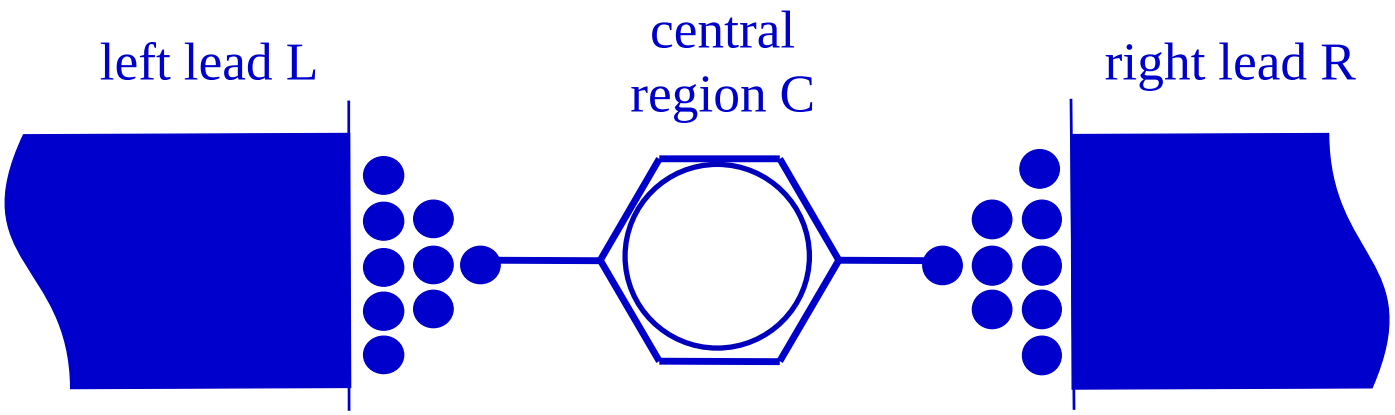

TDKS equation (E. Runge, EKUG, PRL **52**, 997 (1984))

$$i\hbar\frac{\partial}{\partial t}\varphi_j(rt)=\left(-\frac{\hbar^2\nabla^2}{2m}+v_{KS}[\rho](rt)\right)\varphi_j(rt)$$

$$v_{KS}[\rho(r't')](rt)=v(rt)+\int d^3r'\frac{\rho(r't)}{|r-r'|}+v_{xc}[\rho\,(r't')](r\,t)$$

Electronic transport with TDDFT

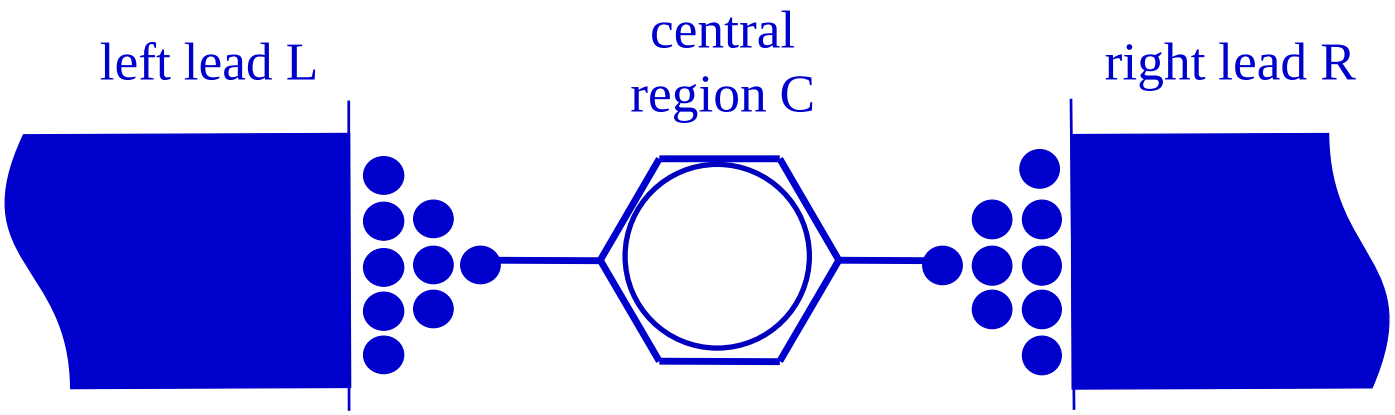

TDKS equation

$$i\frac{\partial}{\partial t}\begin{pmatrix}\varphi_L(t)\\ \varphi_C(t)\\ \varphi_R(t)\end{pmatrix}=\begin{pmatrix}H_{LL}(t) & H_{LC}(t) & H_{LR}(t)\\ H_{CL}(t) & H_{CC}(t) & H_{CR}(t)\\ H_{RL}(t) & H_{RC}(t) & H_{RR}(t)\end{pmatrix}\begin{pmatrix}\varphi_L(t)\\ \varphi_C(t)\\ \varphi_R(t)\end{pmatrix}$$

Effective TDKS Equation for the central (molecular) region only

S. Kurth, G. Stefanucci, C.O. Almbladh, A. Rubio, E.K.U. Gross,
Phys. Rev. B 72, 035308 (2005)

$$i\frac{\partial}{\partial t}\varphi_C(t) = H_{CC}(t)\varphi_C(t) + \int_0^t dt' \left[H_{CL}G_L(t,t')H_{LC} + H_{CR}G_R(t,t')H_{RC}\right]\varphi_C(t') + iH_{CL}G_L(t,0)\varphi_L(0) + iH_{CR}G_R(t,0)\varphi_R(0)$$

source term: $L \rightarrow C$ and $R \rightarrow C$ charge injection

memory term: $C \rightarrow L \rightarrow C$ and $C \rightarrow R \rightarrow C$ hopping

Note: So far, no approximation has been made.

Numerical examples for non-interacting electrons

Recovering the Landauer steady state

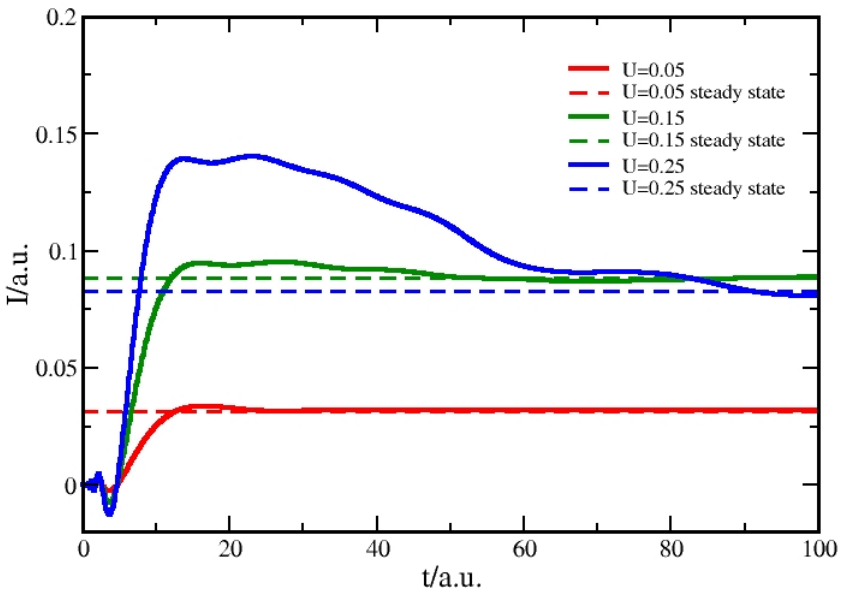

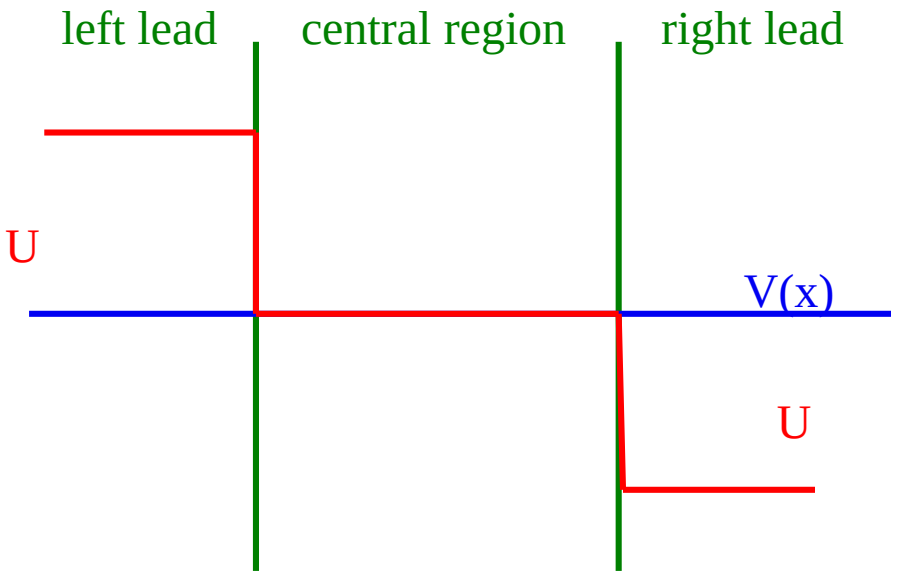

Time evolution of current in response to bias switched on at time t = 0,

Fermi energy $\varepsilon_F = 0.3$ a.u.

Steady state coincides with Landauer formula

and is reached after a few femtoseconds

Can there be more than one steady state?

Multi-stability in TDHF and TDDFT for one-site Anderson model

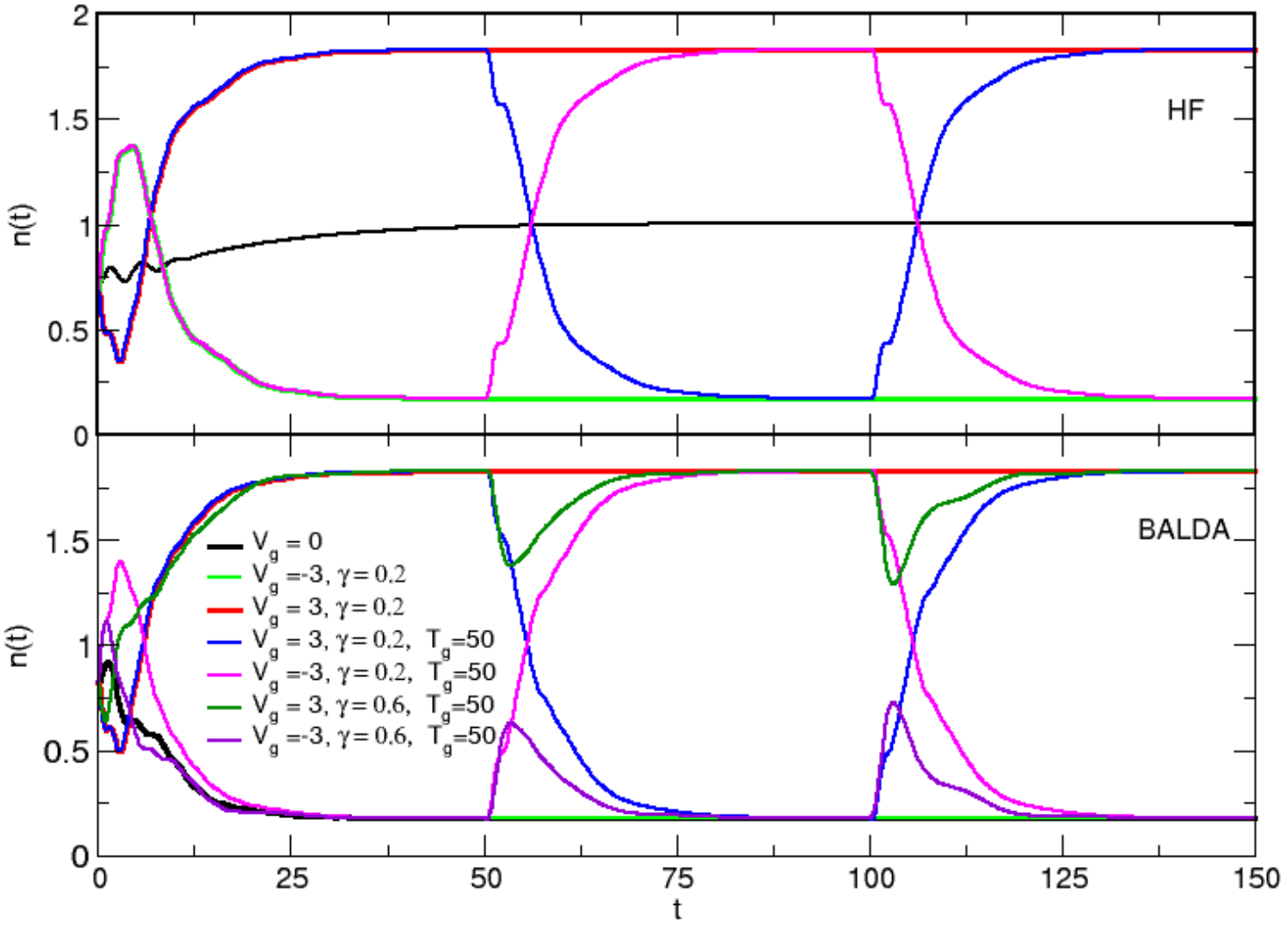

E. Khosravi, A.M. Uimonen, A. Stan, G. Stefanucci, S. Kurth, R. van Leeuwen, E.K.U.G. Phys. Rev. B 85, 075103 (2012)

Is there always a steady state?

No steady state in two-site Anderson model

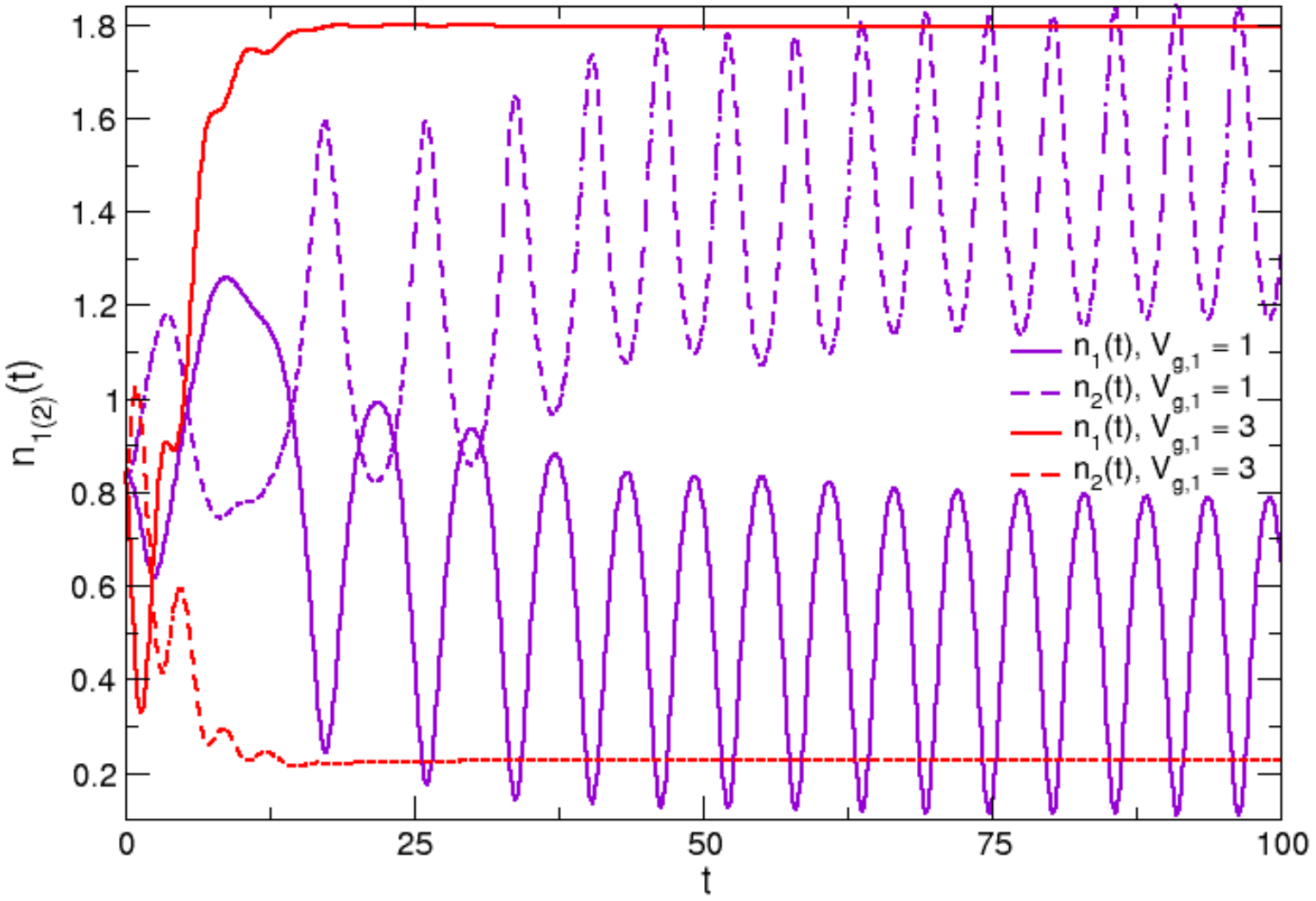

ELECTRON PUMP

Device which generates a net current between two electrodes (with no static bias) by applying a time-dependent potential in the device region

Experimental realization : Pumping through carbon nanotube by surface acoustic waves on piezoelectric surface (Leek et al, PRL 95, 256802 (2005))

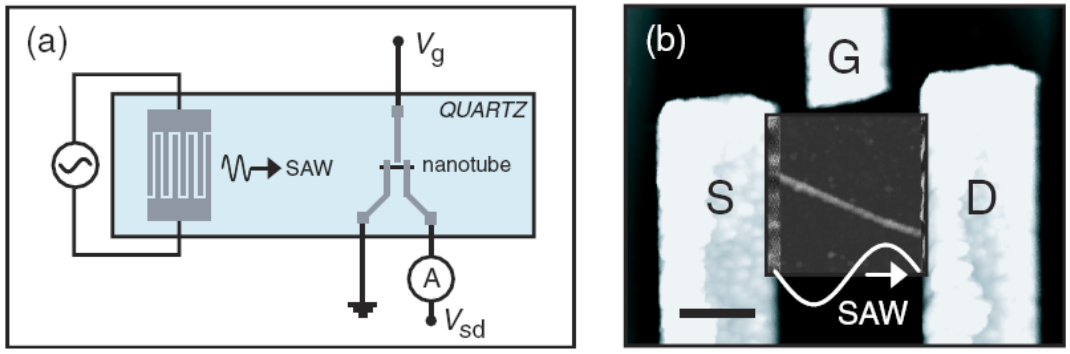

Pumping through a square barrier (of height 0.5 a.u.) using a travelling wave in device region
$U(x,t) = U_o \sin(kx-\omega t)$ ($k = 1.6$ a.u., $\omega = 0.2$ a.u. Fermi energy = 0.3 a.u.)

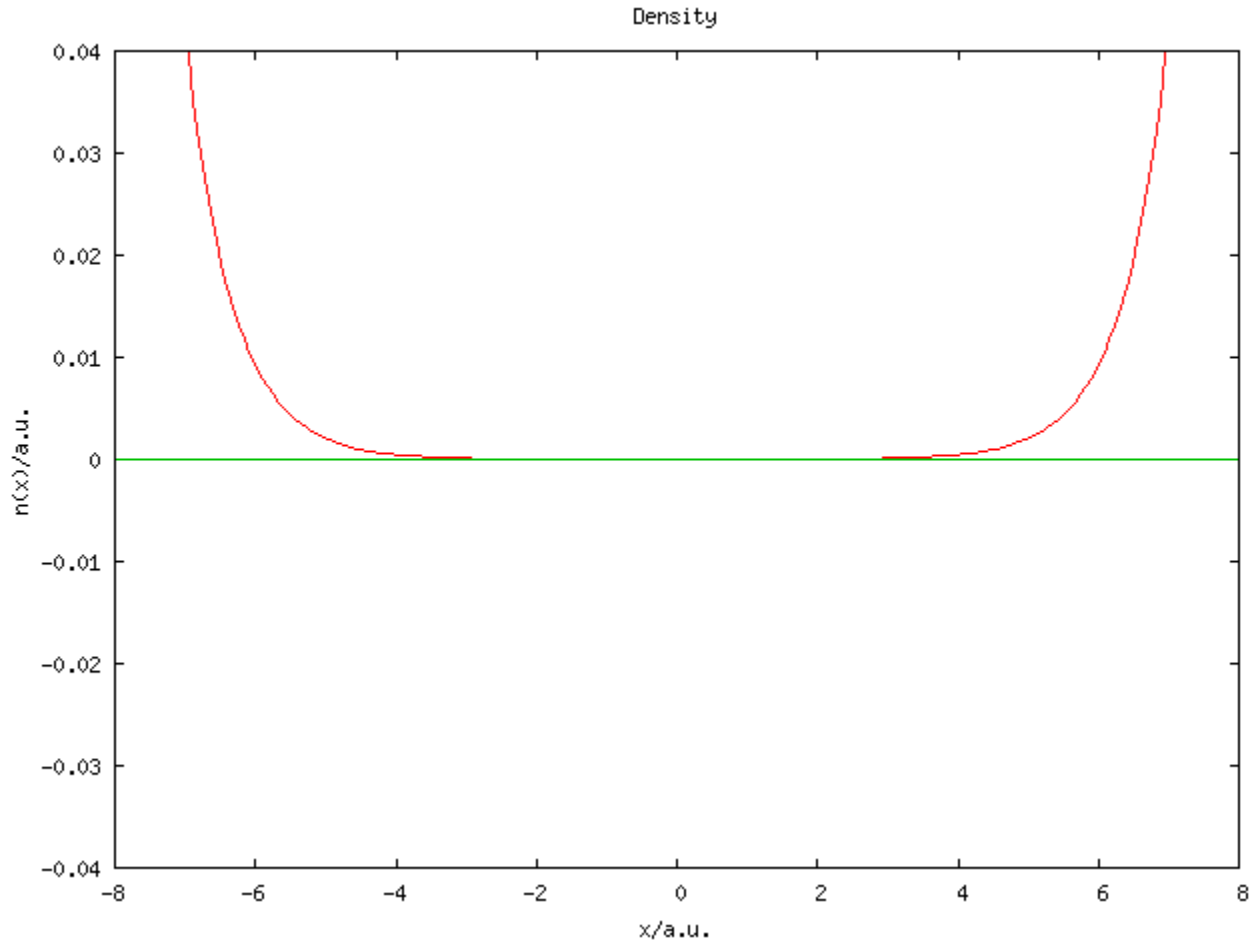

Archimedes' screw: patent 200 B.C.

Experimental result:

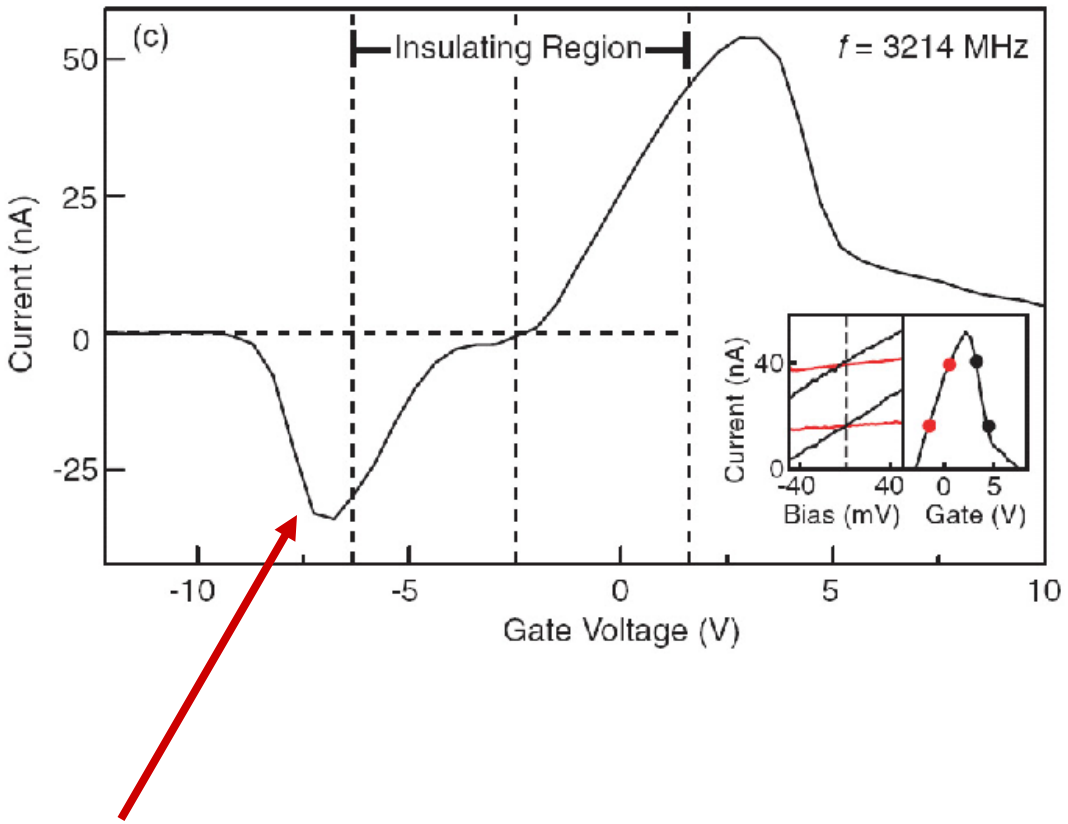

Current flows in direction opposite to sound wave

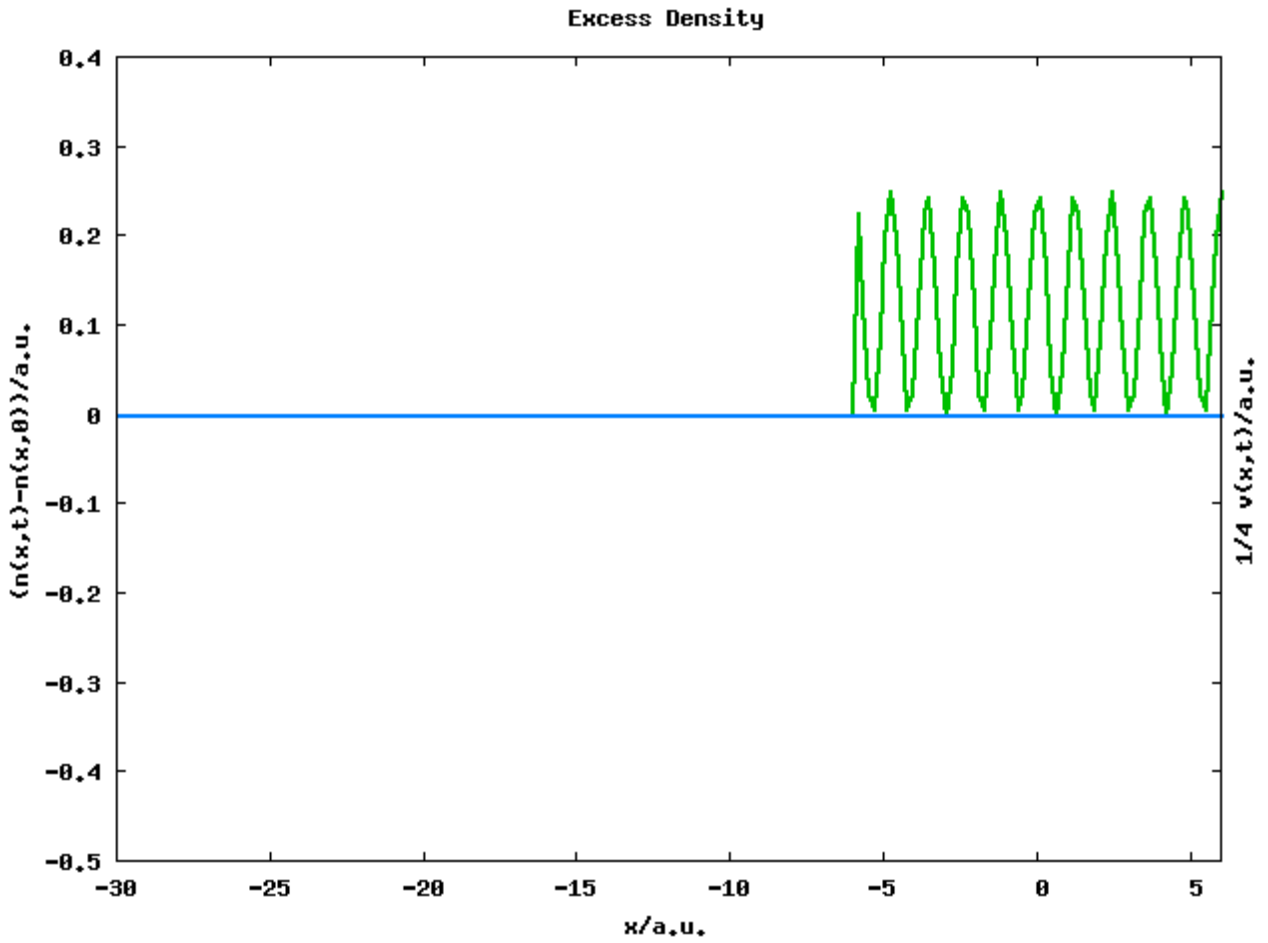
Excess Density
(n(x,t)-n(x,0))/a.u.
1/4 v(x,t)/a.u.
x/a.u.
0.4
0.3
0.2
0.1
0
-0.1
-0.2
-0.3
-0.4
-0.5
-30
-25
-20
-15
-10
-5
0
5

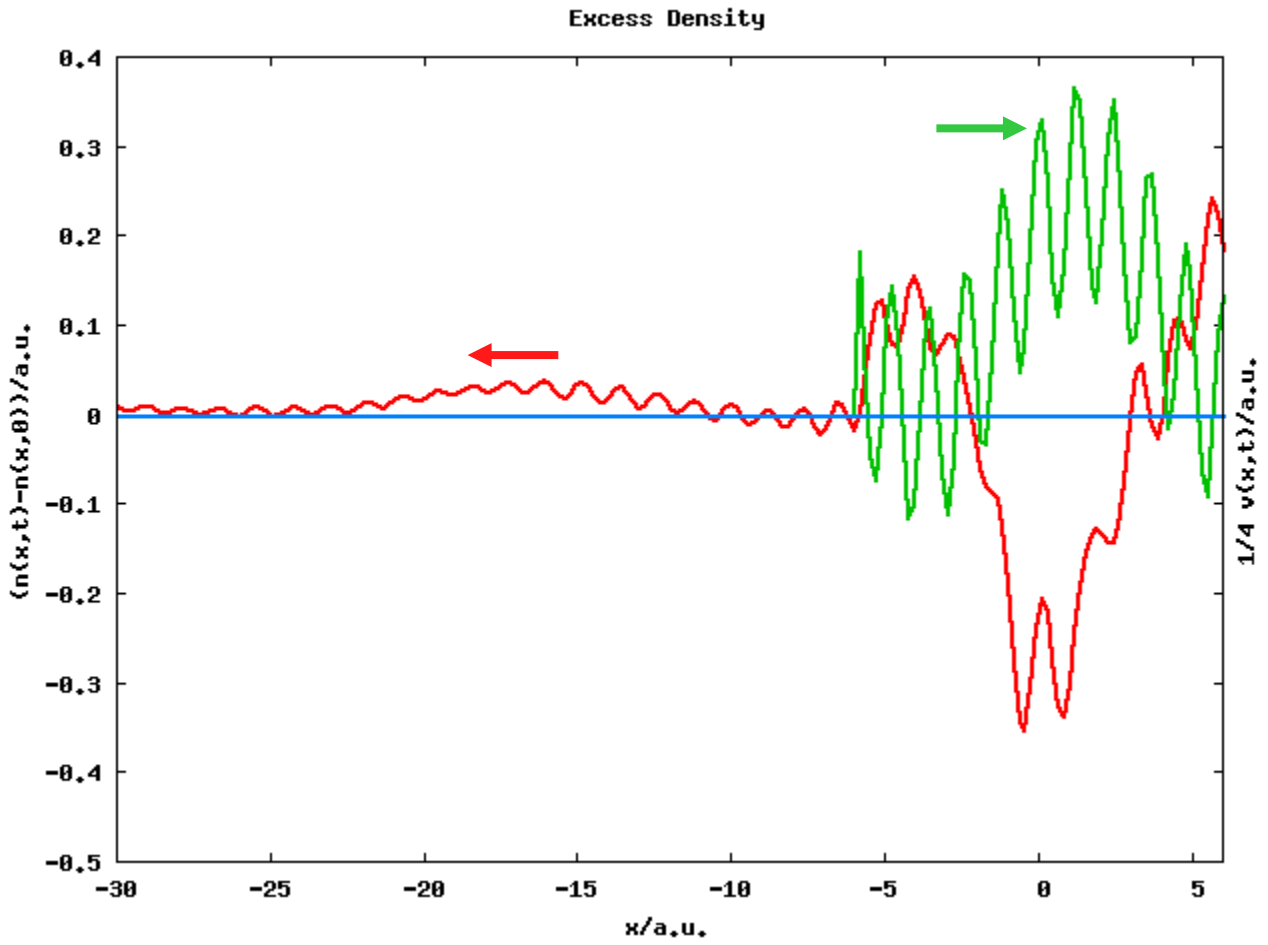

Current goes in direction opposite to the external field !!

G. Stefanucci, S. Kurth, A. Rubio, E.K.U. Gross, Phys. Rev. B 77, 075339 (2008)

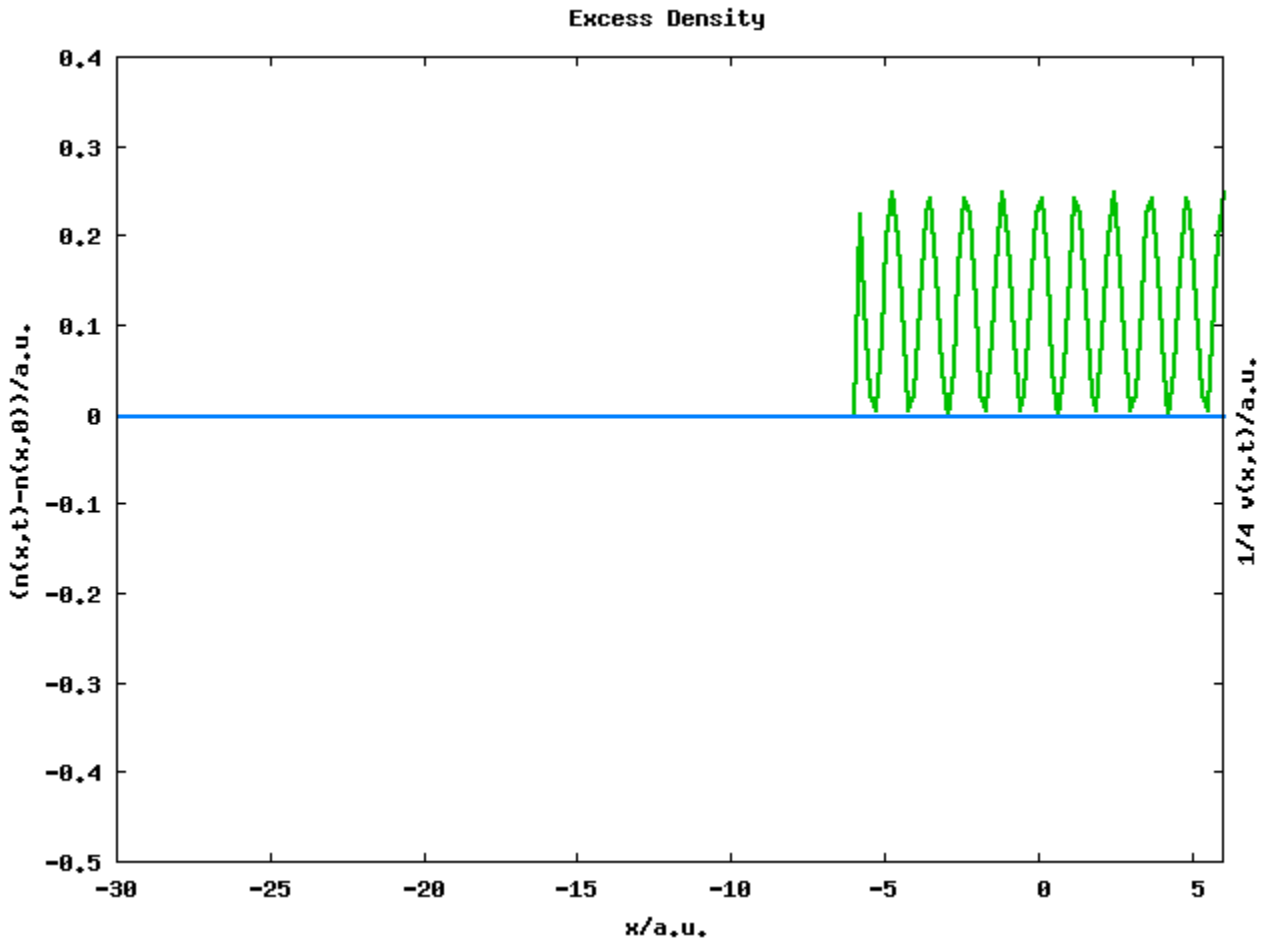

G. Stefanucci, S. Kurth, A. Rubio, E.K.U. Gross, Phys. Rev. B 77, 075339 (2008)

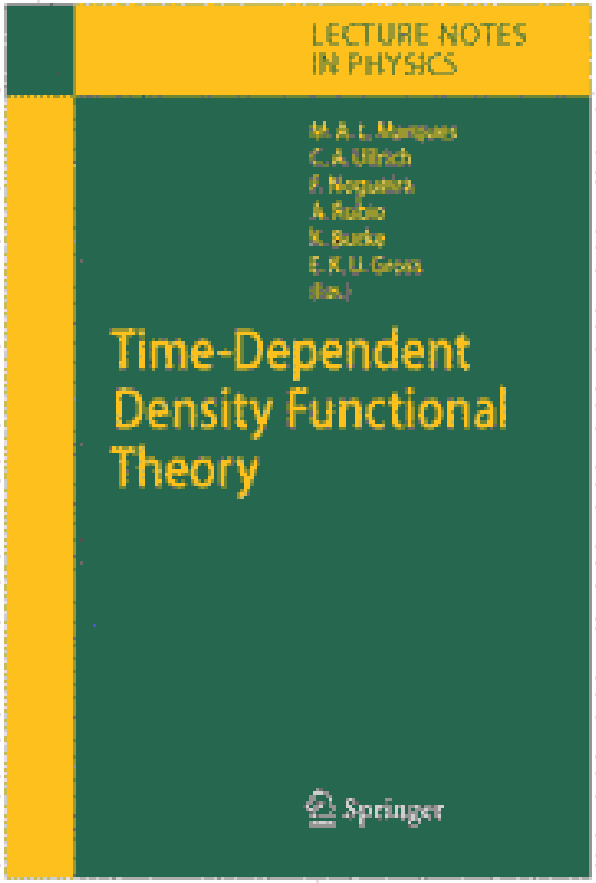

Lecture Notes in Physics 706 (Springer, 2006)

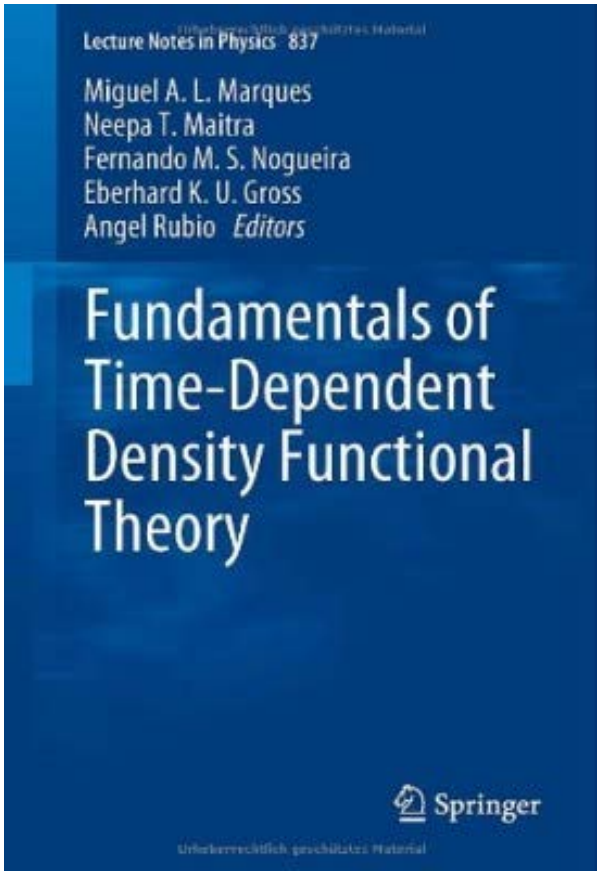

Lecture Notes in Physics 837 (Springer, 2012)